석 . 박사 학위논문 등표지

	Fabrication and Employment of Organic thin films for Organic Light Emitting Diodes • Maria Mustafa • 2014	

A THESIS

FOR THE DEGREE OF DOCTOR OF PHILOSOPHY

Fabrication and Employment of Organic thin films for Organic Light Emitting Diodes

Maria Mustafa

Department of Mechatronics Engineering

GRADUATE SCHOOL

JEJU NATIONAL UNIVERSITY

2014. 02

Fabrication and Employment of Organic thin films for Organic Light Emitting Diodes

Maria Mustafa

(Supervised by Professor Kyung Hyun Choi)

A thesis submitted in partial fulfillment of the requirement for the degree of Doctor of Philosophy

2014. 02

The thesis has been examined and approved.

Ki rin Kwon

Thesis Director: Ki Rin Kwon, Professor, Department of Mechanical Engineering

Yang Hoi Doh

Yang-Hoi Doh, Professor, Department of Electronic Engineering

Seongdai Jo

Jeongdai Jo, Professor, PhD., Korea Institute of Machinery and Materials

Choi Kyung Hyun

Kyung-Hyun Choi, Professor, Department of Mechatronics Engineering

Hong Dong Peoh

Hong Dong Peoh, Professor, Ph.D., Chonbuk National University

Date

Department of Mechatronics Engineering
GRADUATE SCHOOL
JEJU NATIONAL UNIVERSITY

To

My Muslim Sisters

Acknowledgements

Start with the name of Almighty Allah, the most merciful, the most beneficent. First of all I would present my humble gratitude in front of Allah Who enabled me to accomplish the dignified cause of education and learning and I would pray to Him that He would make me able to utilize my knowledge and edification for the betterment of humanity and its development. Most of all, I would like to first express my appreciation to my parents for their encouragement, and endless love. Whenever I am in trouble, their love always guides me on the road of life. I also thank my elder sister and brother for motivating me to continue my studies.

I also thank all my committee members, Prof. Ki Rin Kwon, Prof. Yang-Hoi, Dr. Doh, Jeongdai Jo, and Prof. Hong Dong Peoh for their advice and participation in the review and evaluation of this work.

I again acknowledge Prof. Kyung Hyun Choi for giving me a plenty of chances to test organic electronic devices fabricated by his group, providing access to his students and laboratory equipments. His guidance and expertise allowed me the chance to work efficiently. I also thank Prof. Jeongdai Jo for his advice about my research and attitude for science.

Within the three years of graduate student life in Jeju National University, Jeju, I owe my gratitude to a long list of people. I want to thank all past and current group members Dr. Khalid Rehman, Dr. Nauman Malik, Dr. Naeem Awais, Dr. Naveneethan, Adnan Ali, Muhammad Zubair, Kamran Ali, Murtaza Mehdi, Junaid Ali , Shahid Aziz, Ghayas Siddiqi, Dr. Zahid Manzoor, Hougun Lee, Hyo-Kyun Jeong, Hanna Jo and Jaehee Park.

Contents

List of Figures

List of Tables

Abstract

Organic light emitting diodes based lighting technology is focus of significant academic research and industrial development interest, as they potentially offer unique advantages over their inorganic counterparts in terms of cost reductions, compatibility with low-temperature and printing-based manufacturing. Potential applications of organic light emitting devices span a broad range of products including displays, large area lighting, advertising, information, communication and bio-sensing devices. Although a great progress has been made in this area so far, still requires the search for alternative cost effective fabrication for the development of these low cost organic electronics devices is vital in order meet the demand of industrial large scale production. A wealth of solution processable materials has been synthesized that hold key advantages such as reduced production cost, compatibility with a vast range of substrates such as transparent glass and flexible polymeric materials, and also open new doors to explore alternative low cost fabrication methods.

In this thesis, fabrication methods of functional thin films of organic solution processable materials have been reported and also their deployment for organic light emitting diodes device fabrication from them. Thin films are deposited by electrospray deposition technique in a vacuum-free environment using solution processable materials' inks as precursors. The effects of electrospray process parameters on film's characteristics are described thoroughly. As a means of film characterization, morphology, elemental analysis, optical analysis and current density

analysis for organic light emitting diode device applications are reported. The results obtained have showed that in terms of functionality, the thin films of solution processing materials are suitable to replace their vacuum processed analogues as building blocks in organic light emitting diodes devices. The work opens a fabrication route for a next generation organic electronics device which could lead to important advancement in electronics industry.

1 Introduction

Over the last 40 years, inorganic silicon and gallium arsenide semiconductors, silicon dioxide insulators, and metals such as silver and copper have been the backbone of the semiconductor industry. Silicon is the element central to the microelectronics industry. However, although ideal for many integrated electronics applications, single crystal silicon is not cheap, and the fundamental properties of silicon make it unsuitable for the majority of optoelectronics applications. The use of lower quality amorphous silicon avoids the costs associated with single crystal silicon, and is suitable for cheap information-storing devices like smart cards and inventory control tags. However amorphous silicon requires a glass substrate to "grow" on, which is not exactly ideal for a product to keep in your wallet, or for robust display screens of laptop computers. Furthermore it is still incompatible with most optoelectronic devices. That is why there is a growing scientific movement afoot to build circuits made from entirely new materials – organic plastics. There has been a growing research effort in "organic electronics" to improve the semiconducting, conducting, and light emitting properties of organics (polymers, oligomers) and hybrids (organic–inorganic composites) through novel synthesis and self-assembly techniques. Performance improvements, coupled with the ability to process these "active" materials at low temperatures over large areas on materials such as plastic or paper, may provide unique technologies and generate new applications to address the growing needs for pervasive computing and enhanced connectivity. Review on the growth of the electronics industry clears that innovative organic materials have been essential to the unparalleled performance increase in semiconductors, storage, and displays at the consistently lower costs. However, the majorities of the organic

materials are either used as sacrificial stencils (photoresists) or passive insulators and take no active role in the electronic functioning of a device. They do not conduct current to act as switches or wires, and they do not emit light. But in the late 1970's three scientists (Heeger, MacDiarmid, and Shirakawa) demonstrated that plastic can be made to conduct electricity by manipulating its molecular structure, and shared the 2000 Nobel Prize in Chemistry for their groundbreaking work. Building on their findings, researchers continue to make advances at other institutions such as Lucent's Bell Labs, Cambridge, IBM, Princeton, and Xerox PARC. The shift toward industrial R&D is aided by the establishment of several government-sponsored research initiatives, the founding of various organic electronics driven associations and companies, and the development of IEEE standards for the testing of organic electronics devices. The increased cooperative efforts between academia, industry, and government are vital to the development of a strong materials and manufacturing infrastructure.

1.1 Organic Light Emitting Device

Organic light-emitting device (OLED) based solid-state lighting technology is one the most promising organic electronics based lighting technologies having many superior advantages, such as lower power consumption, having very high in color rendering index, transparent, dimmable, human-friendly, sustainable raw materials, ultrathin, light weight, high contrast, fast response time and large view angle. An OLED consists of very thin layers of organic films sandwiched by two electrodes as shown in Fig. 1-1.

In OLED devices, organic electroluminescent materials, based on π-conjugated molecules, are almost insulators, and light is produced by recombination of holes and electrons which have to be injected at the electrodes. The anode is transparent and is usually made of indium tin oxide (ITO), while the cathode is reflective and is made of low work function metal. The general schematic working principle and energy level diagram of OLEDs is presented in Fig. 1-2 and Fig. 1-3 respectively. When a voltage is applied between the electrodes, injection of holes occurs from the anode and electrons from the cathode. Then, the charges move inside the material, generally by hopping processes and then recombine to form excitons. The location of the recombination zone in the diode is a function of the charge mobility of the organic material as well as of the electric field distribution and is also depend on the thickness of the electroluminescent materials layer (active layer). After diffusion, the exciton recombines and photons are emitted of specific color depending upon the difference between the highest occupied molecular orbital (HOMO) and the lowest unoccupied molecular orbital (LUMO) levels of the electroluminescent molecule. In order to obtain an efficient OLED comparable with the inorganic LEDs, a multilayer stack of active materials is needed, having charge injection, charge transporting and blocking properties.

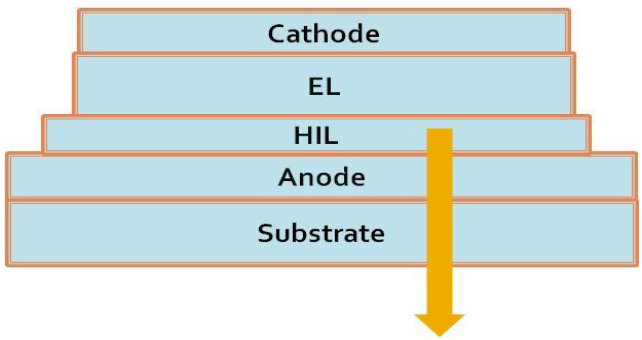

Figure 1-1: Cross section schematic of a typical organic light emitting device.

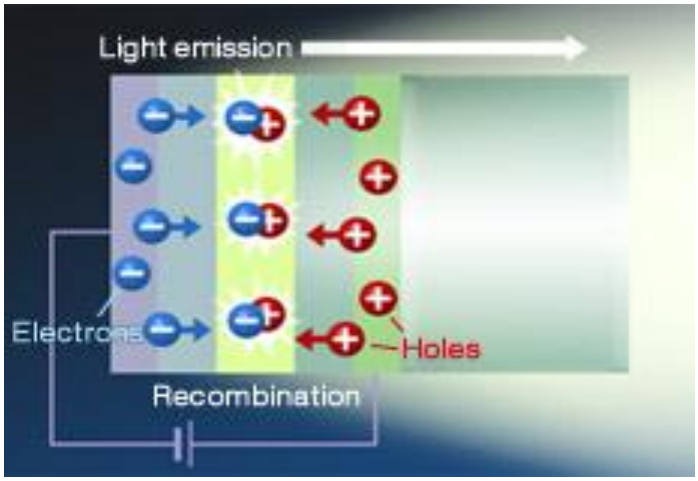

Figure 1-2: Working principle of OLED Device.

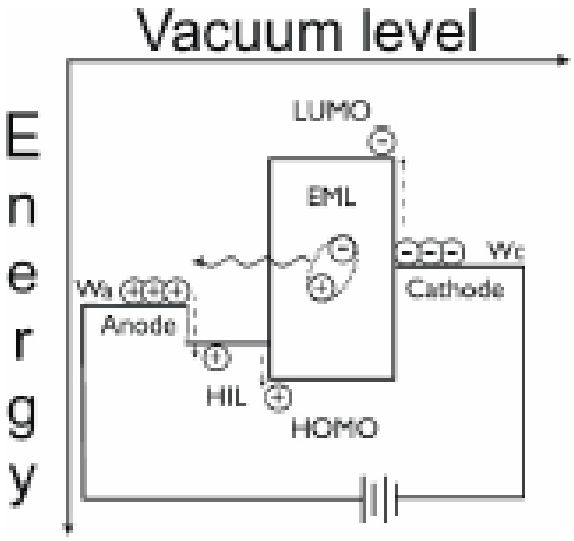

Figure 1-3 Schematic Energy Level Diagram of OLED device.

Organic lighting diodes being emerging class of multidisciplinary research field involves a series of conceptual, experimental and modeling challenging regarding electronic devices incorporating carbon-based materials. The organic light emitting devices are making their way onto market. This new field of electronics in which the structures that are used are based on organic materials: dielectric, conductive or semiconductor polymers or small organic molecules are deposited mainly on flexible substrates.

Figure 1-4: Examples of commercial opportunities for organic electronics.

Organic materials can be made soluble and/or solution processable. This enables a variety of deposition techniques that are not possible for conventional inorganic semiconductor materials. Solution processability enables printing or printing like processes. If one considers (conventional graphic) printing a manufacturing processes, it is easy to realize that it must be one of the highest volume and lowest cost manufacturing processes known. Printing presses commonly run at speeds of hundreds of m/min. with webs several meters wide, and are used to deposit (and cure) many different materials simultaneously. Printing produces large areas very quickly and inexpensively. If one could use these processes (or ones like them) to deposit functional materials, one could produce functional devices in high volume very economically. Such is the appeal of organic electronics. Making this happen, however, will require much effort and development, not only of new materials, but also of thin film processes to be used for these materials. Like most other processes, for optimal performance, the materials will need to be developed with the process and conditions in mind.

Organic light emitting diodes with glass substrate are already used inside the displays of smart-phones. But it is suitable for doing much more with plastic substrate: in the car industry, it serves as an illuminated door sill or to light up the

roof lining, thus providing comfort and a feel-good atmosphere inside the vehicle. OLEDs are suitable for various mobile devices displays such as blood glucose meters or for patient monitoring. The latest applications for organic and printed OLEDs are in e-book readers and touch screens with capacitive sensors. Few examples of OLEDs towards devices applications are shown in Fig. 1-4.

1.2 Promising Materials for Organic Light Emitting Devices

Organic devices rely upon a wide variety of different types of electrically active materials that has ability to process at low temperature sustained by plastic. Among these materials, some of the most commonly used are conductors, semiconductors, dielectrics, as well as various luminescent, electrochromic or electrophoretic materials. Some type of supporting material is generally also used. Much other type of materials can also be employed, such as surface active agents, encapsulation materials, dopants, etc. Brief classification and description of these materials are given below.

Conductors: Almost all printed devices require some type of electrode. The electrodes may need to satisfy a number of requirements including low resistance, smooth surface, chemical stability, and appropriate work function (the energy required for an electron to escape a solid surface) for charge injection into the semiconductor material. The materials used for conductors fall mainly into three categories – those based on metals, organic compounds, and metal oxides. Metallic features can be printed a number of different ways. The most common technique is to use inks that contain metal particles. These particles may span a wide range of sizes and morphologies. Nanoparticles can also be used, and subsequently sintered at plastic compatible temperatures (< 150˚C) to give electrically continuous features.

Metal precursors can also be used, sometimes in combination with other materials, and similarly thermally cured. Another technique that has been used in the printing of conductors is to print a seed layer, followed by plating another metal on top. In this way, printing can be used to define the pattern, and the plating process can be used to deposit a wide variety of metals, often much thicker than what could be printed. The plating process can run at high volume. Even though certain polymers can conduct electricity, they are still > 1000 times less conductive than metals. The compounds that are most used for conductive polymers in printed are hetero-aromatic polymers, based upon aniline, thiophene, and pyrole and their derivatives. Of all of the conducting polymers, the one that has been used the most as a conductor is probably PEDOT:PSS (which is commercially available. Dispersions of PEDOT:PSS have good film forming properties, high conductivity (< 400 S/cm), high visible light transmission, and excellent stability. Films of PEDOT:PSS can be heated in air at > 100˚C for > 1000 hours with only minimal change in conductivity Another class of conductive materials that is often used for electrodes are metal oxides, particularly Indium Tin Oxide (ITO). These materials are used primarily because of their transparency. They are used where transparent electrodes are needed, particularly for light emitting or optoelectronic devices. "They are widely used high- and low-tech applications such as antistatic coatings, touch display panels, solar cells, flat panel displays, heaters, defrosters, and optical coatings". Flexible substrates (polyethylene terephthalate, PET) coated with ITO are commercially available.

Semiconductors: Many organic electronic devices use semiconductors in one or more layers. Frequently, the semiconductor is one of the most critical components,

because it is where the mobile charge carrying species are formed and transported. Semiconducting organic and carbon based materials are currently of broader interest being potential low-cost materials for printable next generation organic electronic applications. The studies of these materials are being carried out extensively in last few years to build devices with a flexibility and softness. On one side materials of polymers has been synthesized and developed day by day and on the other a large focus has been devoted to the exploration of the enhanced properties of the hybrid form of these polymers with inorganic materials. Carbon-based materials are different that conventional in-organic materials like silicon or germanium in many aspects. Usually they are categorized as small molecules and polymers, Polymer semiconducting materials have the electronic properties of semiconductor and can be fabricated with ease of processing in solution phase. The main advantage of the utilization of polymers is their vast applications towards next generation flexible electronic as the curing temperature of these materials are very low. Another important motivation for interest in carbon based semiconducting materials is the expected low cost of the end product of organic devices. Another important motivation for interest in carbon based semiconducting materials is the expected low cost of the end product of organic devices.

It is desirable to have electrical contacts between the semiconductor and the electrodes that are ohmic and have a small contact resistance. Similarly, it is desirable that the material be extremely pure, to eliminate inadvertent sources of traps for the mobile charges. The charge transport in organic semiconductors is highly dependent upon the deposition conditions, and can be influenced by many factors, including solvent, concentration, deposition technique, deposition

temperature, surface treatment, surface roughness, etc. Environmental conditions can also be a major factor, however, some organic semiconductors are air stable and don't require encapsulation or an inert environment to maintain their performance.

For optimal charge transport, the molecular planes should be parallel to each other and as close together as possible. In this situation, the charge will be transported optimally in a single direction (the direction of the intermolecular overlap). In order to make use in a practical device, the direction may also need to be oriented with an appropriate direction in the device, for example, from the source to the drain electrode in a transistor. So not only do the molecules need to be aligned appropriately with each other, they also need to be aligned appropriately with respect to the electrodes.

Many different families of organic semiconductors can be used, including small molecules (pentacene and its derivatives), oligomers (primarily oligothiophenes), and polymers (primarily polythiophenes). A large number of luminescent organic semiconductors (both small molecule and polymer) have also been developed for Organic Light Emitting Diode (OLED) applications. One of the great advantages of organic semiconductors is that it is possible to chemically tailor the structure of the molecule to achieve the desired properties. An important example of this is the use of alkyl side chains to both improve the solubility, as well as to induce molecular ordering, and thereby improve the molecular overlap and charge mobility. In addition to organic semiconductors, nanoparticulate inorganic semiconductors or hybrid organic-inorganic semiconductor materials have also been used. These materials promise both the superior carrier mobility of inorganic semiconductors and the processability of organic materials.

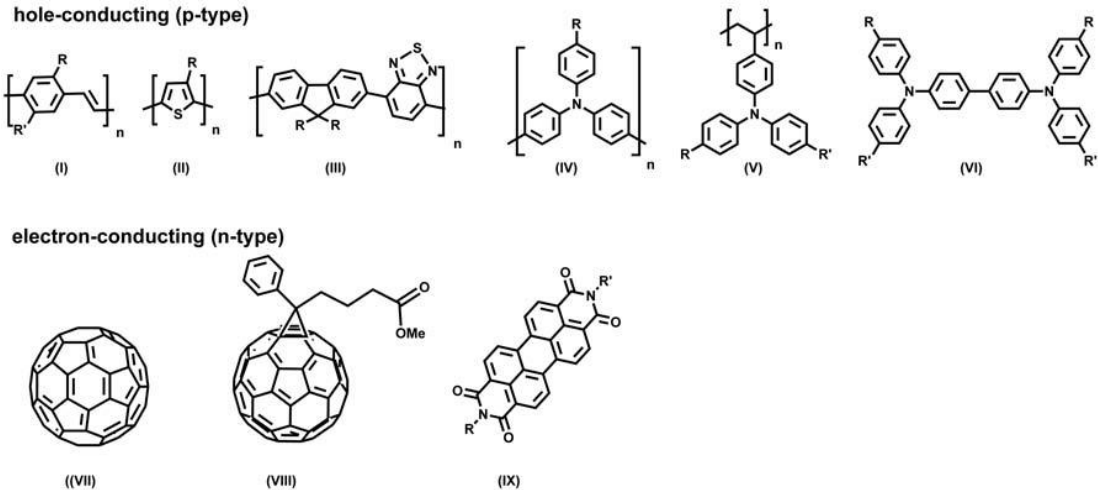

Figure 1-5: Organic hole--(I--VI) and electron--conducting (VII-IX) materials employed for the fabrication of devices: (I) poly(phenylenevinylene) poly[2--methoxy--5--(3,7--dimethyloctyloxy)]-- 1,4--phenylenevinylene) (MDMO--PPV): R':--OMe; R: 3,7--dimethyloctyloxy); (II) polythiophene (poly(3--hexylthiophene) (P3HT): R: hexyl); (III) poly(fluorene--co- benzothiadiazone) (poly(9,9′--dioctylfluorene--co--benzothiadiazole) (F8BT) R: octyl); (IV--V) poly(triphenylamine) (triphenylamine moiety (IV) integrated in the polymer backbone and (V) as side chain); (VI) tetraphenylbenzylidendiamine (TPD); (VII) buckminsterfullerene C60; (VIII) 1--(3--methoxycarbonyl) propyl--1--phenyl[6,6]C61 (PCBM),(IX) disubstituted perylene diimide derivative.

Insulators or Dielectric: In general, a practical dielectric material should have a high capacitance, high dielectric strength, high on/off ratio, high uniformity, high dielectric breakdown, low hysteresis, and be defect free and easily processable. High capacitance is important, because it allows a higher charge density to be induced at lower voltages. This enables the reduction of the threshold and operating voltages, while achieving this at a lower gate field. The capacitance can be increased by using a thinner dielectric or by using a high permittivity insulator material. Unfortunately, when the dielectric layer gets too small, breakdown and reliability issues (defects and yield) can occur. Since the mobility of organic semiconductors is usually fairly low, and the charge transport in organic semiconductors occurs within a few nanometers of the interface between the dielectric and the semiconductor; the properties of the

dielectric, and particularly its surface, are critically important. A variety of materials can be used as dielectrics. While much work has been done using inorganic (silica, alumina, and high dielectric constant oxides) dielectrics, these are not generally printable. A variety of organic polymers including polypropylene, polyvinyl alcohol, polyvinyl phenol, poly methyl methacrylate, and polyethylene terephthalate can also be used as dielectrics. Most of these are polymers that are widely used for non electronic purposes and available in bulk quantities quite inexpensively.

1.3 Fabrication Processes

The outlook for low-cost production of light emitting diode based on organic materials is a key driver for market opportunities in this area. To achieve these cost targets, low-cost materials, cost-effective processes, and high-volume manufacturing infrastructure are required. Organic light emitting diode has a high potential for innovation with regard to the desired production process, printing technology. The development of high-volume roll-to-roll manufacturing platforms for fabrication of organic circuits on continuous, flexible, low-cost substrates, has been reported. Thin organic films compatible to light emitting diode have many attractive features and are being widely investigated for use in electronic devices. The production method is simple, cost-effective and eco-friendly, thus allowing electronic components to be produced in a way which is both ecologically and economically viable. When components are printed using functional materials, an ink made from certain soluble or dispersed functional material is used, which can then be processed in large quantities using common printing processes such as screen printing or inkjet. The organic polymers, which can be used an almost unlimited number of times, can be

printed on a large scale on a wide range of flexible substrates at relatively low temperatures and then integrated into a wide range of products.

In OLEDs, there are three major types of considerations for determining the printing process used. Techniques are chosen based upon their suitability for printing the desired materials (viscoelastic properties), as well as by their capability to print the desired feature sizes (lateral resolution, ink thickness, surface uniformity) required by the device. Economic considerations such as process throughput are also important. The printing processes with the highest resolution capability are also generally those with the lowest throughput (and vice versa). The techniques having a throughput > 1 m^2/sec, are known as "high volume" printing processes. These high volume printing processes are highly desirable to enable the lowest cost production. Solution processed deposition techniques used for thin film fabrication are highly diverse in nature and include spin and spray techniques, Langmuir-blodgett, vacuum filtration and inkjet printing. Different printing processes are discussed individually as follows:

Spin coating: Spin coating is a technique, in which ink is applied to a rotating substrate. The spread of the functional molecules occur due to the lack of centripetal force inward centrifugal forces in the radial direction, thus leaving a fairly uniform layer.

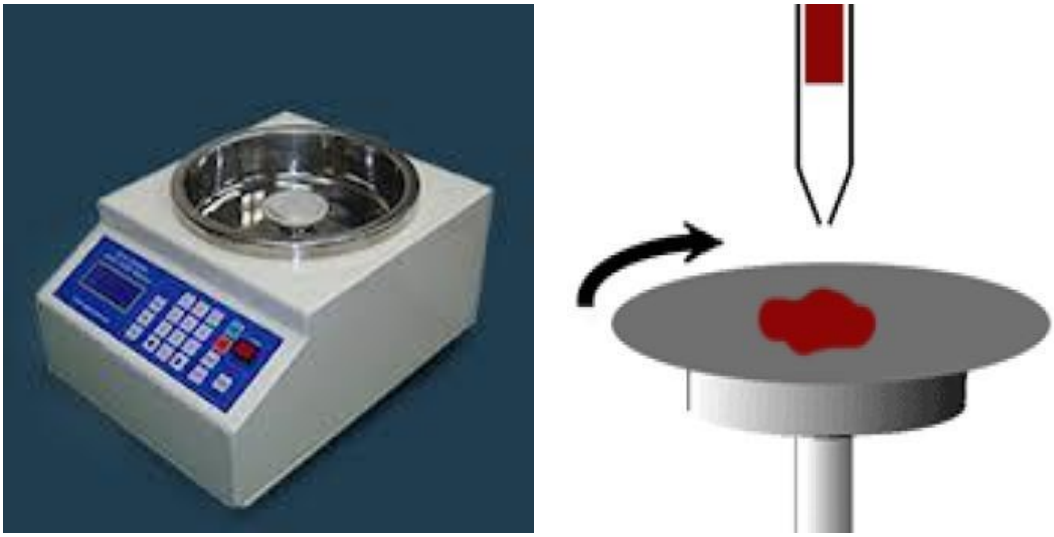

Figure 1-6: Real-time photograph of the Spin coating deposition system and schematic illustration of deposition system.

Screen Printing: Screen printing is a printing technique that uses a woven mesh to support an ink-blocking stencil. The attached stencil forms open areas of mesh that transfer ink or other printable materials which can be pressed through the mesh as a sharp-edged image onto a substrate. A fill blade or squeegee is moved across the screen stencil, forcing or pumping ink into the mesh openings for transfer by capillary action during the squeegee stroke. Basically, it is the process of using a stencil to apply ink onto another material.

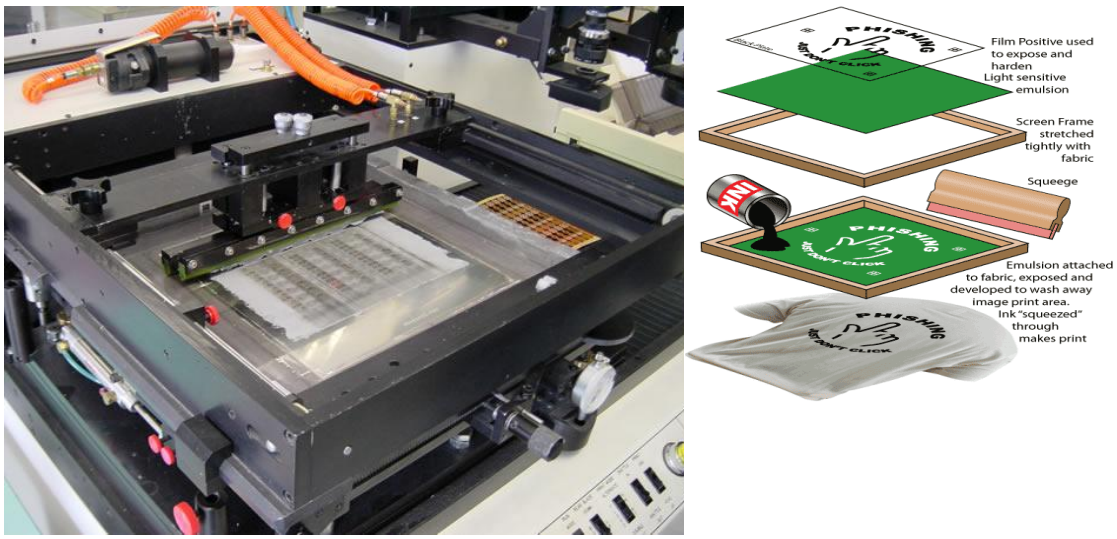

Figure 1-7: Real-time photograph of the Screen printing deposition system and schematic illustration of deposition system.

Screen printing is more versatile than traditional printing techniques. The surface does not have to be printed under pressure, unlike etching or lithography, and it does not have to be planar. Different inks can be used to work with a variety of materials, such as textiles, ceramics, wood, paper, glass, metal, and plastic. As a result, screen printing is used in many different industries.

Langmuir-blodgett technique: With the Langmuir-blodgett technique, the substrate is submerged into the liquid by hand and is pulled from the liquid to air to adsorb a monolayer molecule of functional material, resulted in making the film of micro-dimension on the substrate.

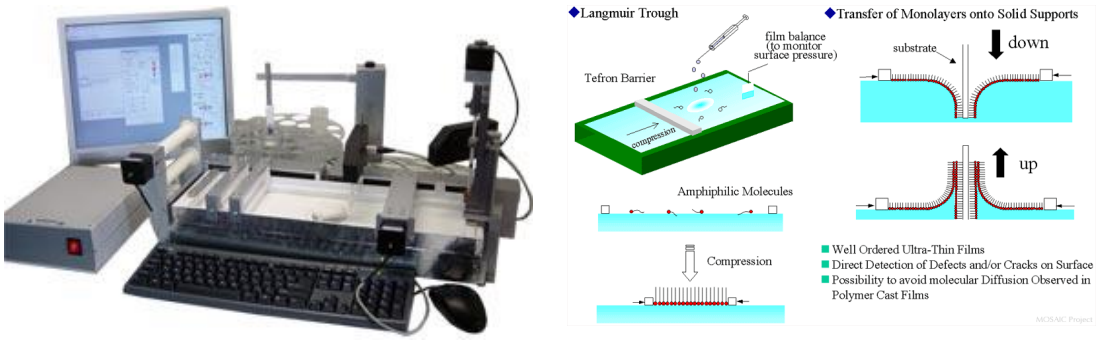

Figure 1-8: Real-time photograph of the Langmuir-blodgett technique deposition system and schematic illustration of deposition system.

Inkjet Printing :Most widely low cost techniques adopted for the fabrication of these solution processed polymers are inkjet printing there by producing highly efficient electronic devices. However in order to make uniform layer structure devices with nanoscale dimensions, these technologies has their own inherent difficulties and limitations with many pitfalls. For these reasons, the development of convenient low cost solution processing techniques has attracted more attention in

the recent years. The most of the above criteria can be met in the method of electrospray deposition.

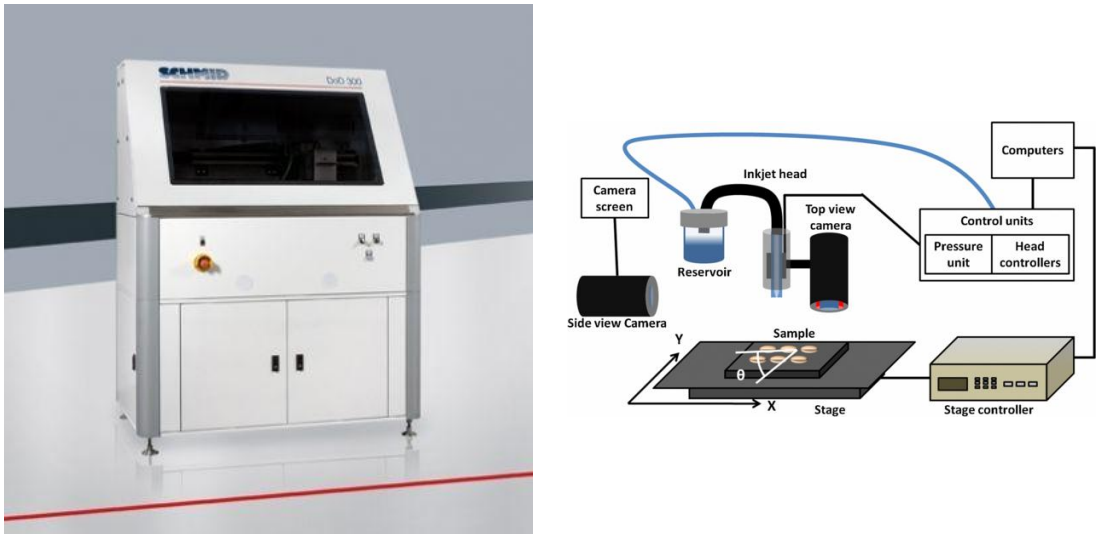

Figure 1-9: Real-time photograph of the inkjet deposition system and schematic illustration of deposition system.

1.4 Electrospray Fabrication Technique

In an EHDA process, the ink containing the functional material is continuously supplied to the metal capillary and is atomized into monodisperse charged droplets of micron size under the influence of the electric field generated on the droplet surface by the application of potential difference (voltage applied) between the nozzle and grounded plate under stable cone jet mode. These droplets of micron size are directed towards the substrate thus making a film of thin dimension on the substrate. Recently, many researchers have applied the EHDA deposition technique to fabricate films of variety of materials on a variety of substrate.

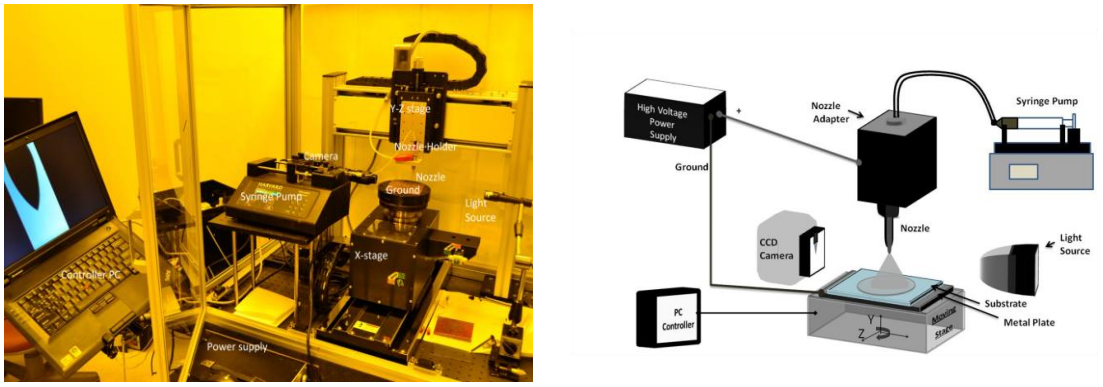

Figure 1-10: Real-time photograph of the ESD deposition system and schematic illustration of deposition system.

Comparing with other solution processed thin film fabrication techniques like spin coating, air brush spray technique and vacuum filtration, EHDA technique has potential to produce high quality nano-dimension thin film for large area coverage thereby meeting the industrial scale up production and high throughput demand using simple setup system. It has ability to produce nano-dimension structures on several types of substrates without causing any type of damage to substrates including flexible and also eliminates the problem of wastage of materials. It provides opportunities for significant cost reduction in existing organic devices as well.

Mechanism of ESD

The thin film fabrication by electrospray generally involved five processes shown in Fig.1-11, which are

(1) Spray formation containing the fine droplets of the precursor liquid;

(2) Droplet transport from the nozzle to the substrate surface accompanied by the evaporation of solvent and possible disruption of the droplets;

(3) The impingement of the droplets on the substrate surface;

(4) The discharge of the impinged charged droplets, the spreading of droplet solution on the surface, the penetration of the solution into the being- formed layer, and a drying process; and

(5) the surface diffusion of solid particles, and physical interaction between these particles [41].

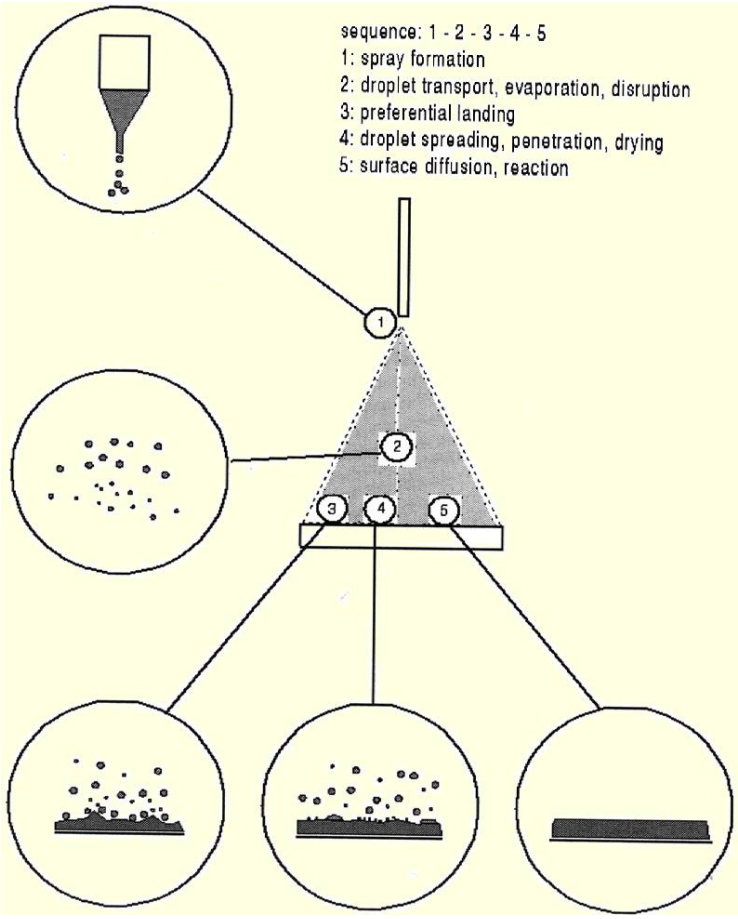

Figure 1-11: Mechanism of thin film fabrication process by electrospray.

Factors affecting the growth, structure and film properties:
Various factors affect the growth, structure and properties of a deposited film.

They are:

(i) nature of the substrate,

(ii) substrate temperature,

(iii) source temperature,

(iv) annealing,

(v) contamination by impurities and presence of defects on the substrate surface, and

(vi) Presence of electrostatic charges etc.

The temperature of the substrate and thickness of the film are two very important parameters affecting its properties. The mobility of the just deposited material on the substrate surface can be enhanced by increasing the temperature of the substrates during the deposition process. Low mobility on the other hand leads to the formation of a film of amorphous nature. If the substrate is the face of a single crystal, periodic forces of cohesion induce an oriented growth called the epitaxial growth. Thus a thin film can be deposited in crystalline, polycrystalline and amorphous form.

1.1 Research Motivation and Thesis Outline

Conventional device fabrication is rather carried out using thin-film materials, which can be integrated and patterned at the nanoscale with relative ease, and whose preparation is cost-effective. The challenge that arises with the use of thin films for nanoscale research and device applications lies, in general, with the greater complexity of the thin-film surfaces relative to bulk materials. Typical thin-film deposition procedures produce thin film surfaces, which normally demonstrate significant topographic roughness on the nanoscale and highly variable atomic-scale texture. For devices where the relevant interactions occur at the atomic and molecular scale, the non-uniform surface structure of conventional thin-film material surfaces can create significant issues for both understanding device behavior and establishing device reproducibility.

To fully realize the potential of nanoscience research to generate device applications — and thus enable the commercial potential of nanotechnology — simple and cost-effective techniques need to be developed for generating uniform and well-

characterized thin-film material surfaces. The research presented in this thesis therefore centers around the fabrication and detailed characterization of organic thin-film material surfaces. The main objectives for the research herein were defined as follows:

1. To develop techniques for fabricating thin-film organic material surfaces of promise for nanoscale research and device applications.
2. To characterize the nanoscale physical and chemical properties of specifically selected thin-film surfaces, chosen because of both their potential utility and the lack of previous detailed examination.
3. To consider future applications in which the determined nanoscale properties of the studied thin-film surfaces could be advantageously employed.

For device applications where organic thin-film material surfaces could be most valuable — specifically, optoelectronics, memories, sensors and nanoscale electronics — the ability to integrate the thin-film surfaces with conventional silicon electronics dramatically enhances the surfaces' potential utility. Based on the above objectives and this criterion, this thesis presents the fabrication and characterization of organic semiconducting materials surfaces that are ultra-thin on the nanoscale. As discussed throughout the thesis, each of these thin-film surfaces fabricated and studied present distinct nanoscale physical and chemical surface properties that are desirable for a variety of nanoscience research and device applications. Furthermore, this selection incorporates representative thin-film having application towards several organic electronic devices — including organic light emitting diode — demonstrating the potential versatility of the fabrication process of ESD technique .

This thesis is structured into two experimental chapters (Chapters 2 and 3). Each chapter examines a specific process for fabricating ultra-flat thin-film, and includes the detailed characterization of at least one material of particular interest. The layout of each chapter generally follows the sequence of the objectives listed in the previous section. The start of every chapter provides general background on the ultra-flat thin-film surface fabrication technique and particular surfaces explored therein, along with the impetus underlying the selection of both for study. The film formation processes are then presented, in conjunction with any experimental data relating to process development. The experimental characterization of the select thin-film surfaces follows next, along with the experimental characterization of other related surfaces incorporated for comparison where appropriate.

2 Fabrication of Organic Thin Films

2.1 Poly [2-methoxy-5-(2'-ethylhexyloxy)-(p-phenylenevinylene)] Thin Film

Conjugated polymer materials have been getting enormous attraction in polymer based organic optoelectronic devices due to their efficient optoelectronic properties as well as the ease of processing in solution phase [M. Kertesz et. al; 2005, C. Zhong et. al; 2011, H. Spanggaard et. al; 2004]. On one side materials of polymers has been synthesized and developed day by day [L. Zhao et.al.; 2011, T.W. Yoo et. al.; 2011, A. Swinarew et.al.; 2011, O. Lavastre et. al.; 2004, P.R. Andres et.al.; 2004] and on the other a large focus has been devoted to the exploration of the enhanced properties of the hybrid form of these polymers with inorganic materials [J.A. Ayllon et.al.; 2009, S. Kumar et.al.; 2004, A. Petrella et. al.; 2005, R. Taylor et. al.; 2007, C. Ton-That et. al.; 2008]. The main advantage of the utilization of polymers is their vast applications towards next generation flexible electronic as the curing temperature of these materials are very low.

MEH-PPV polymer has been intensively studied because of its broad applications in organic devices. MEH-PPV is characterized by a pi-conjugated backbone in which the pi-electrons are delocalized over several monomer units along the carbon chains, forming pi-bands. Because the delocalized orbital are half filled, the energy gap between the filled and empty bands results in semiconducting properties. The extent of delocalization of the pi-electrons, the so called conjugation length, determines the energy gap, which plays a major role in the optical and electrical properties of the materials and the performance of the organic devices they are used in.

Most widely low cost techniques adopted for the fabrication of these solution processed polymers are inkjet printing [J. Bharathan et. al.; 1998, S.C. Chang et. al.; 1998, S. C. Chang et. al.; 1999, B.C. Krummacher et. al.; 2006, Y. Liu et. al.; 2003, K.E. Paul et. al.; 2003], spin coating [T.S. Kang et. al.; 2003; N. Rehmann et. al.; 2007, S.A. Arnautov et. al.; 2004, W. Lee et. al.; 2008], there by producing highly efficient electronic devices. However in order to make uniform layer structure devices with nanoscale dimensions, these technologies has their own inherent difficulties and limitations with many pitfalls [J. Sidén et. al.; 2007, S. Di Risio et. al.; 2007, S.A. Jenekhe et. al.; 1984, W.W. Flack et. al.; 1984, K. Jong Lee et. al.; 2006, S. Ilkhanizadeh et. al.; 2007]. For these reasons, the development of convenient low cost solution processing techniques has attracted more attention in the recent years.

Electrospray deposition (ESD) has been extensively studied and investigated as an alternative method for achieving the fabrication of thin films of valuable materials [S. Jayasinghe et. al.; 2004, A. Van Zomeren et. al.; 1994, P. Miao et. al.; 2001, D.H. Youn et. al.; 2009, A. Khan et. al.; 2011, A. Gupta et. al.; 2007, R. Bakhshi et. al.; 2009, A. Khan et. al.; 2011, N.M. Muhammad et. al.; 2011, J. Ju et. al.; 2009]. In the electrospray deposition process, an electric field is applied to a pendant droplet of the precursor containing liquid solution generated at the tip of the metallic nozzle by applying the potential difference of the order of kilovolts between the metallic nozzle and the grounded electrode. The droplet thus deforms into a conical shape, with a filament emanating from apex, known as cone-jet transition and then at particular distances below the nozzle, this filament fans out in the form of the spray of charged particles. These charged particles are attracted towards the substrate

that is being connected to the grounded electrode there by forming a thin film [H.F. Poon et. al.; 2008, R. Hartman et. al.; 2006, K. Rahman et. al.; 2010, K.H. Choi et. al.; 2010, O.V. Kim et. al; 2010, I. Hayati et. al.; 1986, T. Nguyen et. al.; 2001]. The thin film fabrication by electrospray deposition technique generally involves five processes which are (i) spray formation containing the fine droplets of the precursor liquid; (ii) droplet transport from the nozzle to the substrate surface accompanied by the evaporation of solvent and possible disruption of the droplets; (iii) the impingement of the droplets on the substrate surface; (iv) the discharge of the impinged charged droplets, the spreading of droplet solution on the surface, the penetration of the solution into the being- formed layer, and a drying process; and (v) the surface diffusion of solid particles, and physical interaction between these particles [H.F. Poon et. al.; 2008]. The main advantages of ESD technology for the fabrication of thin film include the possible tailoring of the morphology of the deposited film [S. Gil Kim et. al.; 2000, N.M. Muhammad et.al.; 2011] and high deposition efficiency since the electric field direct the charged droplets to the substrate with a very simple setup architecture[N.M. Muhammad et. al.; 2011, T. Nguyen et. al.; 2001, S. Gil Kim et. al.; 2000, N.M. Muhammad et.al.; 2011, K.H. Choi et. al.; 2011]. Prior to ESD, the basic understanding of electrostatic spray of liquid solution need to be investigated in order to fabricate the high quality thin film.

In this study, the understanding of electrostatic atomization of the in-house developed ink was made by using ESD technology, followed by fabrication of the thin polymer films. Polymer investigated for electrostatic atomization was poly[2-methoxy-5-(2'-ethyl-hexyloxy)-1,4-phenylenevinylene] (MEH-PPV) and was selected because it is one of the most popular conjugated polymers and has been

utilized extensively in many electronic devices [M. S. P. Sarah et. al.; 2010, N. Kamarulzaman et. al.; 2011]. The operating envelope of ink was explored. Then the thin film of polymer was prepared and was thoroughly characterized using different thin film characterization tools. The surface morphology inspection was performed by using JEOL JSM-7600F Field Emission Scanning Electron Microscope (FESEM) machine operated at the accelerating voltage of 5 kV. For film thickness measurement, thin film thickness machine K-MAC ST4000-DLX was used. The surface roughness analysis was done by using PAFM S100 Atomic Force Microscope (AFM). To look into elemental composition of the film, X-ray Photoelectron spectroscopy (XPS) of the film was conducted using VG Microtech XPS analysis equipment equipped with a monochromated X-ray source. Base pressure during analysis was 1×10^{-7} Pa. For electrical characterization, the Agilent B1500A Semiconductor Device Analyzer coupled with MST8000C Probe Station having a current resolution of 1fA was used. Prototype organic diode devices with structure of Indium Tin Oxide (ITO)/ Poly(3,4-ethylenedioxy-thiophene):poly(styrenesulphonate) (PEDOT:PSS)/ MEH-PPV were fabricated with electrosprayed and spin coated MEH-PPV layers on Polyethylene terephthalate (PET) separately. Then electrical characterization of diode devices was performed by current voltage measurement and was compared.

2.1.1 MEH-PPV Polymeric Thin Film Deposition

MEH-PPV (Avg. Mol wt: 51000) powder and ITO coated PET substrate was purchased from Sigma Aldrich company. The PEDOT:PSS (2.8% wt) (Orgacon) was supplied by Agfa Materials Japan Limited, Japan. The N, N-dimethyl-formamide

(DMF), Di-cholorobenzene (DCB), acetone and ethanol was purchased from Daejon Chemical and Metal Co. Ltd., South Korea.

The solution having 0.4% of MEH-PPV concentration was prepared by dissolving appropriate amount of MEH-PPV powder into the DCB solvent. Then the solution was subjected to stirring for 24 hours at the temperature of 80 ˚C. In order to get powder completely dissolved, the solution was given the bath-sonication treatment for 200 minutes maintaining the temperature of 60˚C. The polymer solution was then allowed to cool to room temperature and was filtered using 0.2 µm syringe filters. At the end, DMF solvent was added into the ink with the composition ratio of 1:3 of that of polymer solution. The resultant ink was then used for ESD process. The viscosity value of the ink was measured by Viscomate VM-10A and it was recorded to be 2.5 mPa. The surface tension measured from SEO's contact angle analyzer was 27 mN/m. The dielectric value measured from BI-870 Dielectric Constant meter was 19.2. The electrical conductivity of the ink was measured by Conductivity meter (Cond6+ meter) and its value was 2.5 µS/cm. The viscosity of the ink was kept low in order to avoid electro-spinning phenomena induction [I.B. Rietveld et. al.; 2006, C.H. Park et. al.; 2009].

The electrostatic atomization of MEH PPV ink was attempted using ESD system [N.M. Muhammad et. al.; 2011]. The brief description of the system was as follows: the ink solution was placed in the chamber (Nano NC Nozzle adapter) through syringe pump (Hamilton, Model 1001 GASTIGHT syringe) and was provided at constant rate to the nozzle through the syringe pump. The metal nozzle of 210 µm internal diameter [Havard 33G] was used as anode and was connected to a Trek Model 610E high voltage source for the generation of required electric field. Ground

was provided by connecting the ground terminal of the power source to the moving stage and the substrate was placed on this moving stage. The speed of moving stage was kept at 3 mm/sec. A high speed camera along with a light source was used in conjunction with a portable computer to capture images of the electrostatic atomization events. The flow rate with combination of voltage was used in order to observe different modes of electrostatic atomization. The ink was subjected to electrostatic atomization at 5 kV and 450 µl/hr under the stable cone jet mode. After that, the distance between the capillary and the substrate was varied between 12 mm to 23 mm in order to find the optimized distance followed by fabricating the film keeping all other parameters of ESD constant. An ITO coated PET was used as substrate and was cleaned with ethanol, acetone and deionized water respectively for 15 min each, dried and was subjected to spray. The resultant sample thus prepared was thermally cured at 100 ˚C for 5 hours and was further used for surface morphology analysis in order to investigate the quality of the film at each standoff distance there by evaluating the optimized ESD parameters. By using optimized parameters, the MEH-PPV thin films are prepared to observe the surface roughness and thickness of the films. The samples on bare glass with slight different parameters were also prepared and were used for single film XPS analysis, and electrical measurement.

2.1.1.1 Ink Characterization and Spray Formation

The electrostatic atomization of the ink was investigated for the identification of an operating envelope that can adopted while fabricating the thin film for the particular electronic device applications. The electrostatic spray was first performed with varying flow rate from 50 µl/hr to 450 µl/hr in order to determine optimum the spraying envelope. At each flow rate, the strength of electric field was increased by

gradually increasing the potential difference between the anode nozzle and the grounded stage [K. Rahman et. al.; 2010, K.H. Choi et. al.; 2010]. By varying the potential difference, various modes of electrohydrodynamic phenomenon were observed from dripping to multi-jet mode. Figure 2-1 shows the high resolution and high speed images of different spray modes as achieved at different value of potential differences keeping flow rate constant at 150 µl/hr. At zero potential difference, dripping mode was only observed. Then the potential difference was gradually changed from zero to 3.1 kV, only micro-dripping was observed. As the potential difference was further increased, a pulsating cone jet was observed at 4.1 kV. Then at potential difference value of 4.6 kV, a stable cone jet was witnessed which remained until around 5.9 kV after that the multi-jetting was started. If the applied potential difference was further increased, the jet discharged. A flow rate of 450 µl/hr has been selected for the film fabrication. This value is selected as the droplet has directly dependence on flow rate. However if the flow rate is too low, the stable cone jet formation is going to be unstable after sufficient time span [N.M. Muhammad et. al.; 2011]. Figure 2-2 provides the observed optimum operating envelope of the developed ink representing various atomization zones with varying flow rate and their corresponding potential difference values.

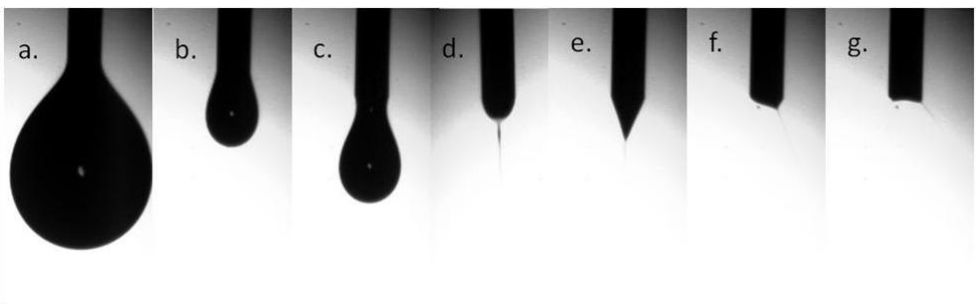

Figure 2-1: Mode of Electrostatic atomization of MEH-PPV ink; a) dripping, b) & c) micro dripping, d) pulsating unstable cone jet, e). stable cone jet , f) un-stable jet, g.) multi-jet cone.

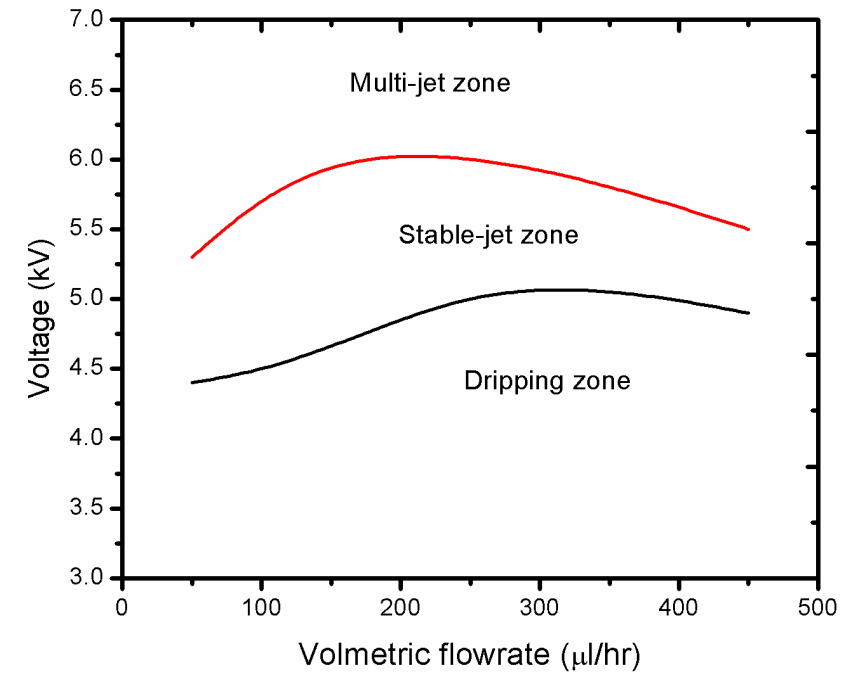

Figure 2-2: Figure 3: Operating envelope of polymer ink.

The inequalities between electrical relaxation time (T_q) and hydrodynamic time (T_h) are a perquisite for the well established atomization phenomenon. The value of electrical relaxation time must be much smaller than that of the hydrodynamic time. Both T_q and T_h depends on the ink properties as well as the on the ink jetting behavior. At the flow rate of 150 µl/hr, the diameter of jet was 10µm and length of jet was 600µm. With these values and the ink parameters, the value of T_q and T_h came out to be 7.977×10^{-6} and 1.4×10^{-4} respectively using the empirical relations [N.M. Muhammad et. al.; 2011], which showed that the ink was satisfactory fulfilling the criteria of electrical atomization.

2.1.2 Thin Film Characterization

2.1.2.1 Structural Analysis

The standoff distance is one of the important parameters of ESD technology and has direct effect on the quality of the thin film. It determines the time of solvent evaporation when droplet travel towards substrate. To see the effect of the stand-off distance on the film quality, the electrostatic spray process was carried at four different standoff distances of 12 mm, 15 mm, 20 mm, and 23 mm. The samples thus prepared were subjected to SEM analysis. Figure 2-3 shows the effect of standoff distances on the film morphology. At a standoff distance of 12 mm, the film was highly porous and could be resulted due to the fact that the high amount of solvent travelled down to the substrate and after drying left behind a large amount of empty spaces on film. At the standoff distance to 15 mm, the quality of the film got improved. The film was in the form of semi-liquid, and was not showing any wetting problems, the solution flow or the rough grainy formations problem. It could be easily seen at distance 15 mm that the quality of the polymer film was satisfactory and free of pores. As the standoff distance was further increased, the pores started appearing again and the quality of film become unsatisfactory. At this distance, the film was formatted as a result of the evaporation of the most of the solvent during the droplet flight causing to disturb the optimum ratio of polymer and solvent necessary to form smooth film as well as restricting their spreading. The quality of film went worse as the distance reached at 23 mm. An optimum distance from nozzle to substrate was determined to be 15 mm at which the resulting film quality was satisfactory.

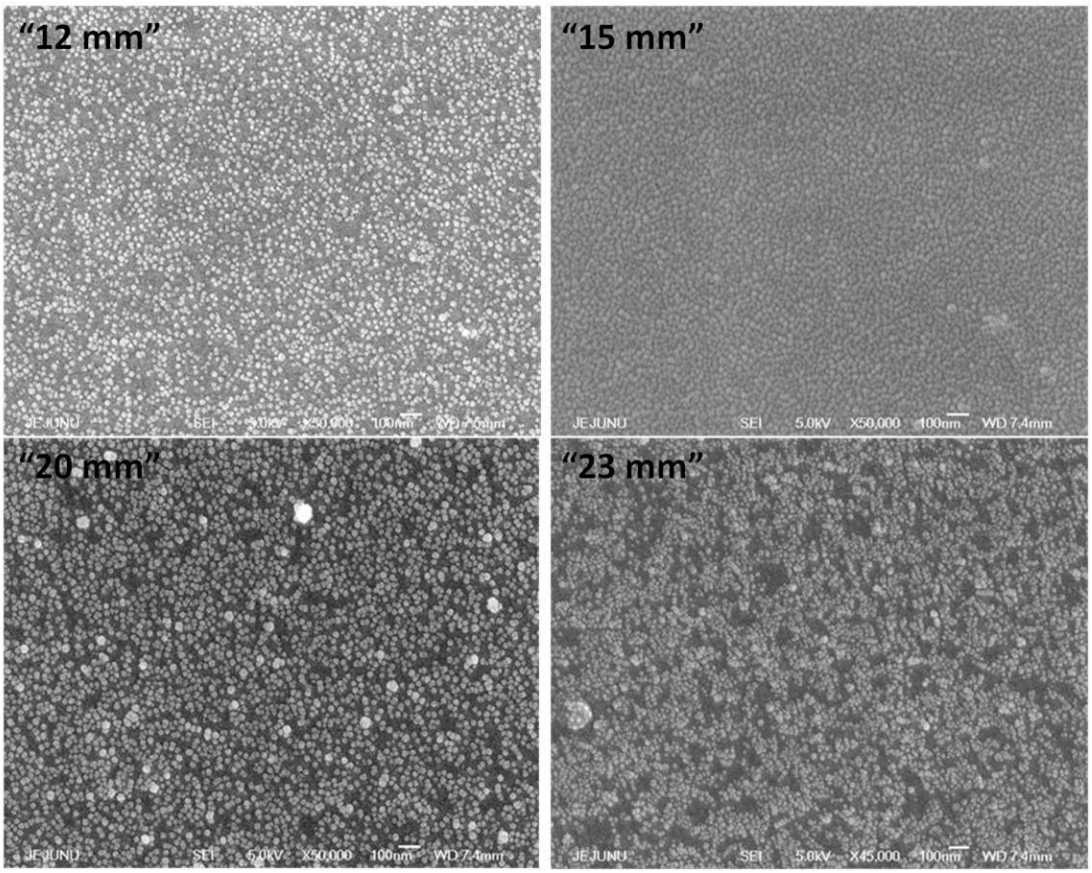

Figure 2-3: SEM images of the MEH-PPV thin films deposited at a standoff distance of 12, 15, 20 and 23 mm.

The surface roughness of the film was investigated by atomic force microscopy. The AFM image over 100 μm x100 μm scan area was shown in Fig. 2-4. The AFM image shows a smooth surface with the RMS value of 11.5 nm hence can be utilized in electronic device manufacturing.

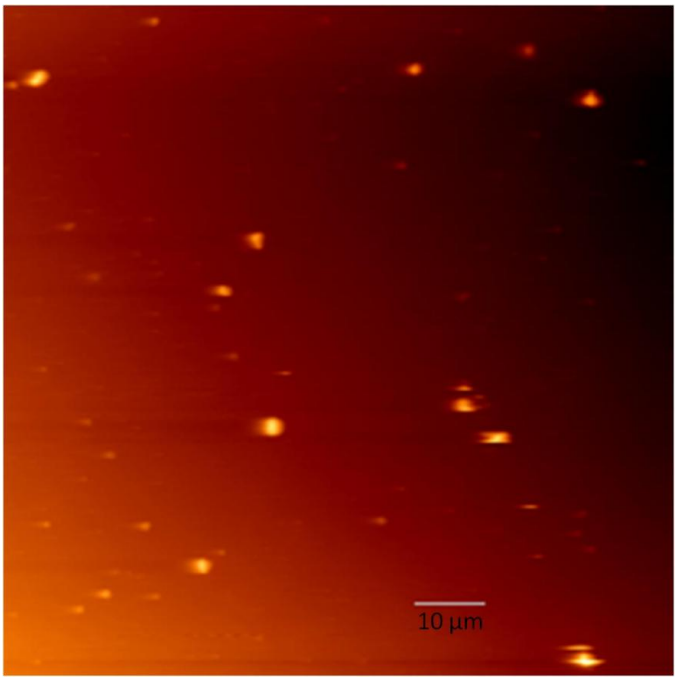

Figure 2-4: AFM image of the MEH-PPV thin film deposited by electrospray.

The average thickness of the MEH-PPV film measured by film thickness machine was 168 nm ± 20 nm which is acceptable for the nanoscale electronic devices.

2.1.2.2 X-ray Photoelectron Spectroscopic Analysis

One of the issues related to electronic failures is the presences of solvent that remain within the layers of electronic device during fabrication [S. Li et. al.; 2000]. In order to confirm the complete removal of the solvent, the XPS survey spectrum analysis of the electrospray deposited MEH-PPV film on glass was carried out and was shown in Fig. 2-5. The figure indicates two prominent peaks which are ascribed to C and O elements [S. Huang et. al.; 2011, A. Ltaief et. al.; 2004].

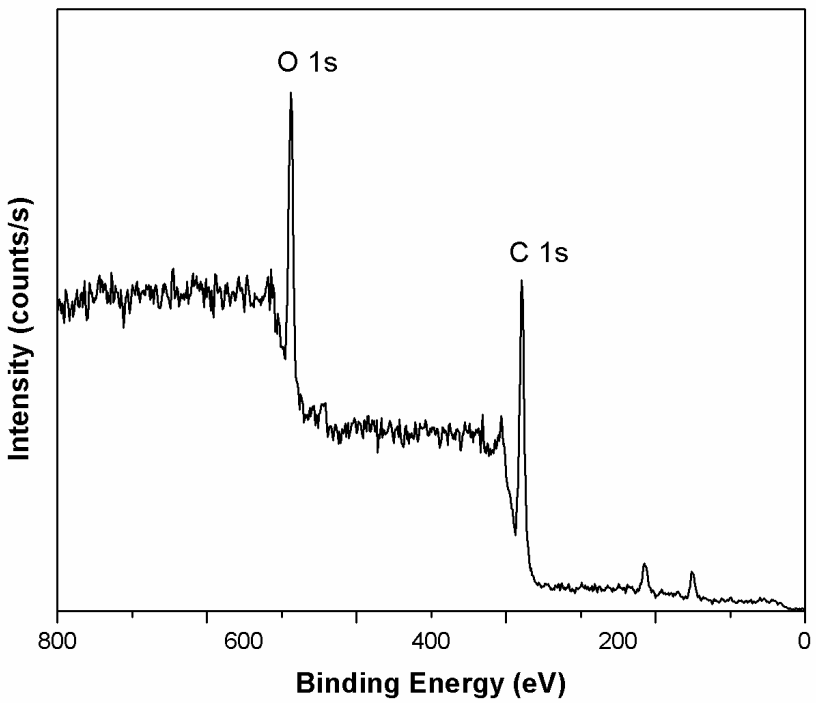

Figure 2-5: The XPS survey spectrum of MEH-PPV film deposited by ESD technique.

2.1.2.3 Optical Analysis

Figure 2-6 shows the absorption spectra of electro sprayed MEH-PPV thin films within UV-visible range. MEH-PPV thin film gave broad peak above 350nm centered at 495 nm wavelength which is associated to non-localized states (HOMO-LUMO transition) [A. Marletta et.al; (2004)]. Overall the result suggests that the films of MEH-PPV polymers show good optical properties.

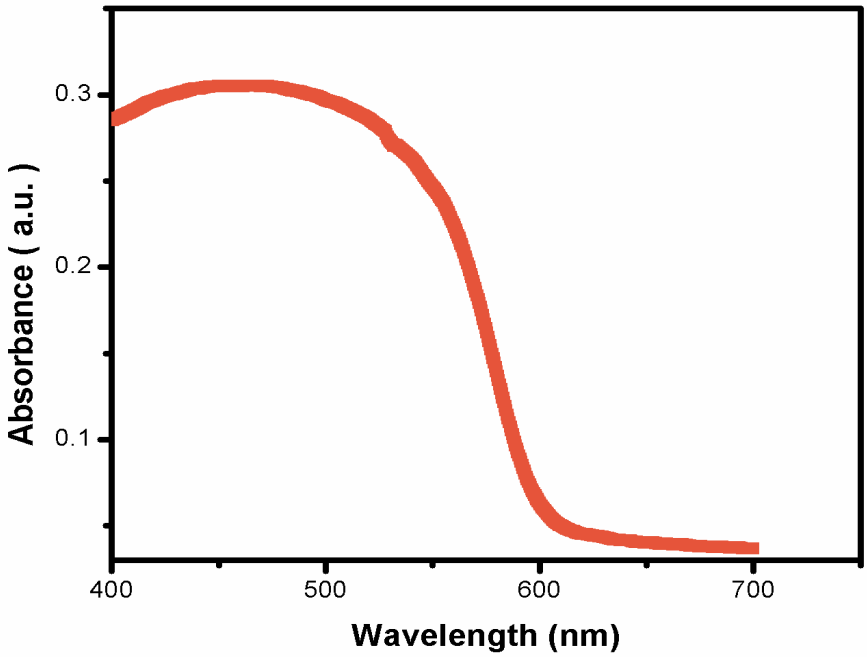

Figure 2-6: Absorption spectra of annealed MEH-PPV onto ITO coated PET.

2.1.2.4 IV Analysis

In order to measure the conductivity of the polymer thin film, IV characteristic curve for the single layer of electrosprayed MEH-PPV was recorded as shown in Fig. 2-6(i). From the IV curve, the conductance of the film was evaluated. Here the IV curve was presenting the semiconductor like behavior of MEH PPV deposited film and the conductance of the film is calculated to be 7.14×10^{-5} Ω^{-1} which accords with that found in literature [M. S. P. Sarah et. al.; 2010, N. Kamarulzaman et. al.; 2011]

After the electrospray process was optimized, an ITO/PEDOT:PSS/MEH-PPV organic diode was fabricated. The feasibility of electropsray for the multi-layered structured diode was analyzed through its electrical characterization using semiconductor analyzer. For the comparative evaluation with spin coating process, a

diode of same electronic structure was developed with spin coated MEH-PPV film having comparative thickness to that of electrosprayed polymer layer and its electrical performance was analyzed and compared.

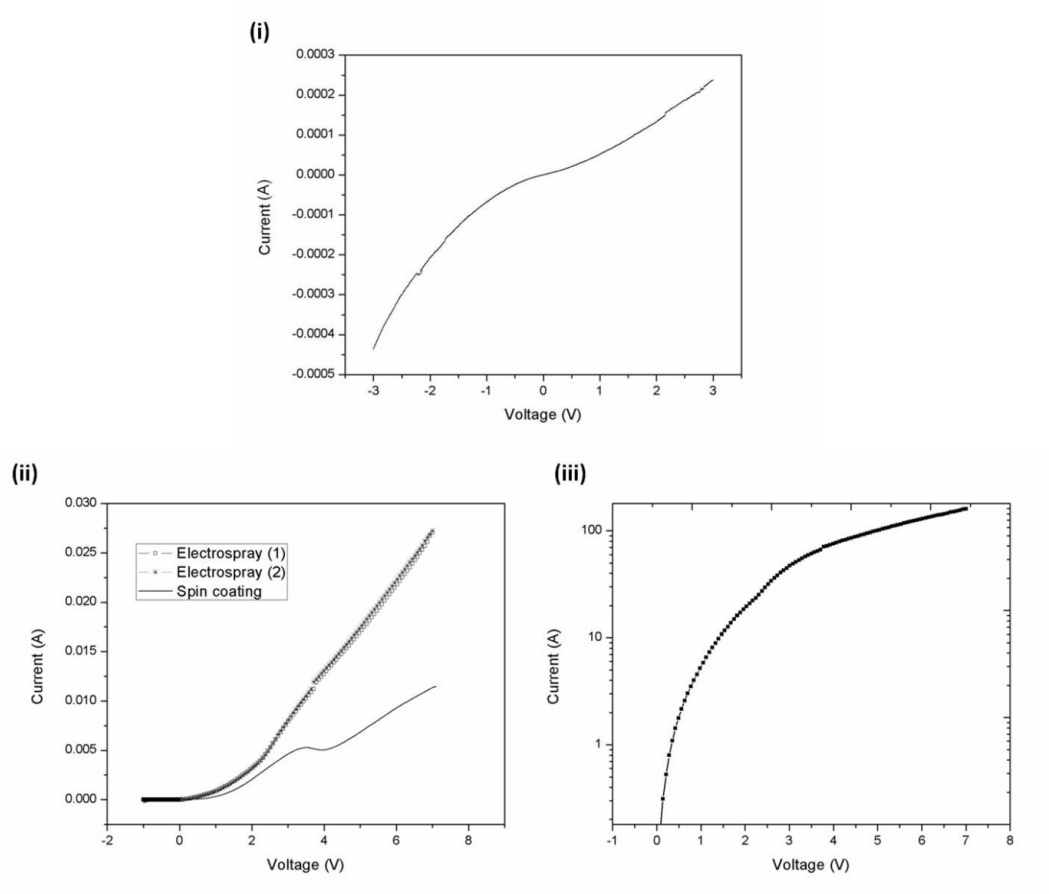

Figure 2-7: (i) IV characteristics of MEH-PPV single layer deposited on glass substrate, (ii) IV characteristics of ITO/PEDOT:PSS/MEH-PPV organic diode in linear scale and (iii) IV characteristics of ITO/PEDOT:PSS/MEH-PPV organic diode in semilograthimic scale.

Electrical behavior of the multi-layer film is very much dependent on the contact of the two adjacent films and plays an important role in the performance of the electronic device. The IV curve of the organic diode structures in linear scale, recorded by semiconductor analyzer was shown in figure 2-7(ii) with electrosprayed as well as spin-coated MEH-PPV layer. It is clear from the figure 2.7(ii) that the

diode structure with sprayed MEH-PPV polymer film shows better performance. For voltage 5 V, the current in organic structure with spin-coated polymer film is 7×10^{-3} A versus current in sprayed one, reaching about 1.6×10^{-2} A there by indicating the proper contact area of the uniformed electrosprayed layer with adjacent film in the diode structure and resulting in increase charge carrier injection efficiency. The organic diode having electrosprayed MEH-PPV film, showed typical Schottky diode like behavior having a barrier height of 0.68 eV and ideality factor of 1.57 as evaluated from the semilogarithmic plot of IV curve of the organic diode shown in Fig. 2-7(iii). The experiment with electrospray deposition technology was repeated in order to check the reproducibility of the process as shown in Fig. 2-7(ii). A relatively small deviation (average 0.23 mA) was observed. The reason behind this deviation is as the encapsulation of the structure was not performed, so there is possibility of the impact of contamination from the environment on the electronic structure performance which will be well thought-out as a part of future work.

2.1.3 Conclusions

In conclusion, the electrospray atomization of polymer ink has been achieved there by fabricating defect free MEH-PPV nano scale thin layer. The effect of standoff distance on the film morphology was investigated and optimized to the value of 15 mm. The film of polymer fabricated by optimized ESD parameters was thoroughly examined. The e-spray deposited MEH-PPV film showed the absorption edge at wavelength of 495 nm. The electrical behavior of the thin polymer was that of semiconductor nature showing a conductance of $7.14\times10^{-5}\,\Omega^{-1}$. Contact between the two adjacent polymers layers in organic diode structure with electrosprayed MEH-PPV film was quite satisfactory compared to that of the organic diode with the spin

coated MEH-PPV layer as evident from the IV characteristic curve of organic diodes. The reproducibly of the electrospray process towards organic diode fabrication was evaluated and was found satisfactory. OLED device with thin electrosprayed MEH-PPV emissive layer show good current transporting anad electroluminance properties because of proper contact between the adjacent layers in OLED structure. Overall the results achieved highlights electrospray deposition as a key and promising technology in the production of polymer nano thin films for organic diode structures in environmental friendly manner.

2.2 Poly[9,9-dioctylfluorenyl-2,7-diyl]-co-1,4-benzo-(2,1,3)-thiadiazoleThin Film

The development and commercialization of polymer semiconductors have made revolutionary progress due to the rapidly growing demand for printed electronic applications [J. M. Shaw et.al; 2001]. Being low temperature and solution processable, polymer materials have been gaining considerable interests to develop organic electronic devices for future printable electronics [P. Leclere et. al; 2006, M. Friedman et. al.; 2002]. Among them, the conjugated polymer poly[9,9-dioctylfluorenyl-2,7-diyl]-co-1,4-benzo-(2,1,3)-thiadiazole (F8BT) has attracted much attention because of its high long alkyl side chains that are introduced to increase solubility and its wide band gap [L. L. G. Justino et. al.; 2009]. Furthermore it is relatively stable in air and its physical properties have been extensively studied [M. Campoy-Quiles et. al.; 2005, S. Cook; 2003, J. K. Grey et. al.; 2006, C. R. McNeill et. al.; 2006]. F8BT based devices has found their applications in the field of organic light emitting diode lighting and display electronics [D. Kabra et. al.; 2010], organic transistor technology development [L. L. Chua et. al.; 2005, S. A.

DiBenedetto et. al.; 2009], photovoltaic cells [S. Westenhoff et. al.; 2008], and in the high-speed optical data communication systems [B. Wenger et. al.; 2010].

Historically, conjugated semiconducting polymer molecules were mainly deposited by vacuum deposition techniques since they showed limited solubility in common solvents [C. W. Tang et. al.; 1987, J. C. Wittmann et. al.; 1991, H. Ichikawa et. al.; 2005, M. Prelipceanu et. al.; 2007]. However, some drawbacks of vacuum based film fabrication have also been reported [T.P. Nguyen et. al.; 2006]. Besides this, for large substrate coverage there is a need to adopt fabrication technique that has mechanical flexibility, and has huge potential for monolithic integration of different organic devices onto one common substrate in cost effective fashion. With the significant progress in development of the organic materials, the polymers are made compatible with the solution processed fabrication methods. The most popular cost effective thin film fabrication methods that come under the category of solution processed technique are wet processes and include a dip-coating, a screen printing, and a conventional spin-coating [T. Ito et. al.; 2001, J. Jiang et. al.; 2006, S. Jeong et. al.; 2004, M.-Y. Lee et. al.; 2010]. One serious problem of these solution processes is the dissolution of the under layer, and it makes difficult to prepare multilayer structures formed by different polymer layers using a conventional wet process. Recently, many spray techniques have been developed to deposit organic multilayer films [X. Zhao et. al.; 2008, G. Susanna et. al.; 2011, J. M. Bharathan et. al.; 1998, S. C. Chang et. al.; 1998, S. C. Chang et. al.; 1999, B. C. Krummacher et. al.; 2006, Y. Liu et. al.; 2003, K. E. Paul et. al.; 2003] and these methods are suitable to fabricate organic devices with satisfactory performance.

However, the smaller size of droplets of the polymer solution while spraying is important for further improvement in the surface quality and the device performance.

Electrostatic spray (E-spray) technique is the efficient liquid atomization process that has been used widely to fabricate the functional materials' thin films. In this method, the high voltage approximately of several kilo volts is applied to the precursor solution containing functional material and solvent and cause the solution to divide into micron-size droplets [I. Hayati et al.; 1986]. As the droplets flight towards substrate, the solvent is partially evaporated before reaching the substrate, and the thin film of functional material is deposited just like a thermal evaporation method without dissolving the under organic layer. Other interesting features of this technique are the simple experimental setup without special vacuum conditions and the possibility of achieving multilayer architecture of thin films with high uniformity and good morphology [I. Hayati et al.; 1986, H. F. Poon et. al.; 2002]. This technology has been adopted to deposit variety of functional materials for various industrial applications [I. Hayati et al.; 1986, H. F. Poon et. al.; 2002, R. Hartman et. al.; 2000, O. V. Kim et. al.; 2010, A. A. V. Zomeren et. al.; 1994, P Miao et. al.; 2001, S. N. Jayasinghe et. al.; 2004, L.-C. Chao et. al.; 2008, D. H. Youn et. al.; 2009, A. Gupta et. al.; 2007, R. Bakhshi et. al.; 2009, J. Ju et. al.; 2009, A. Khan et. al.; 2011, A. Khan et. al.; 2011, N. M. Muhammad et. al.; 2011, K .Rahman et. al.; 2010, K. H. Choi et. al.; 2010, N. M. Muhammad et. al.; 2011, K. H. Choi et. al.; 2011, N. Duraisamy et. al.; 2012]. E-spray approach has been adopted for fabrication of F8BT polymer thin films in the past but need further improvement in a manner of optimization of parameters of fabrication process [T. Fukuda et. al.; 2009].

This study presents the fabrication of solution processed F8BT thin film with evaluated optimized e-spray process parameters. Ink was synthesized in-house and was subjected to electrostatic atomization under the influence of applied electric field. The operating parametric envelope of the ink was explored. After that, the thin film fabrication was carried out followed by annealing of the film. The surface morphological analysis of the resultant films was performed in order to observe the quality of the films fabricated at different spray parameters. The elemental composition of the polymer film was confirmed by X-ray Photoelectron spectroscopy analysis and then optical characterization was carried out at room temperature. After the optimization of e-spray process parameters, the attempt was made to fabricate the organic diode device having e-sprayed F8BT as an active layer. The performance of organic was analyzed by performing current voltage measurement at room temperature.

2.2.1 F8BT Polymeric Thin Film Deposition

The F8BT polymer powder (Avg. Mol wt: 10,000) and ITO coated PET substrate were purchased from Sigma Aldrich, South Korea. The PEDOT:PSS (Orgacon) was supplied by Agfa Materials Japan Limited, Japan. The dimethyl sulfoxide (DMSO), tetrahydrofuran (THF), acetone and ethanol solvents were purchased from Daejon Chemical and Metal Co. Ltd, South Korea.

A schematic diagram of e-spray system is shown in the Fig. 1-7 [A. Khan et. al.; 2011, A. Khan et. al.; 2011, N. M. Muhammad et. al.; 2011, K .Rahman et. al.; 2010, K. H. Choi et. al.; 2010, N. M. Muhammad et. al.; 2011, K. H. Choi et. al.; 2011, N. Duraisamy et. al.; 2012]. At first, the F8BT solution was made by dissolving F8BT powder in THF solvent at a content of 0.3g/ml at room temperature. To have good

quality film, the mixed-solvent approach was adopted in making an e-spray ink [J. A. Lim et. al.; 2008] using DMSO and added to the F8BT solution in ratio of 1:10. The resultant polymer solution was stirred for 1hr at room temperature and was placed in a 1-ml glass syringe mounted in the syringe pump (Harvard Apparatus, PHD 2000 Infusion). From the syringe, solution was supplied to nozzle adapter (nozzle holder) through teflon tubing and from there, a continuous ink supply was given to the stainless steel metal nozzle (O.D 340μm). The nozzle adapter was connected to a high voltage source capable to generate DC voltage up to 30kV. A substrate was placed on a flat moving stage whose motion is controllable by the computer under the metal nozzle. A ground was given to this moving stage. The flow visualization of solution under electric field was recorded by a high resolution CCD camera (Motion Pro X) along with a light source connected to the computer. The distance between the nozzle and substrate (standoff) was varied keeping all other parameters of e-spray process constant in order to check its effect on the surface morphology of the thin film. The operating envelope for ink was explored by varying the flow rate between 300 μl/hr to 1000 μl/hr and raising the voltage gradually from 0 kV to upto 6 kV.

After that, the glass substrates were bath-sonicated with acetone for 15 min followed by rinsing it with deionized water and finally dried at room temperature. After that, the deposition of F8BT layer was performed on them with the flow rate of 400 μl/hr under the condition of stable cone jet mode. For continuous film fabrication, the speed of the moving stage was set at 3 mm/sec and the number of deposition passes was varied. The resultant samples were sintered at 100 ºC for 30 min and were then characterized by using different thin film characterization tools.

For organic diode fabrication, the ITO coated PET substrate was cleaned and was oxygen plasma treated for 1 min. After that, the deposition of PEDOT:PSS as hole injection material was performed. For that, a layer of PEDOT:PSS of thickness of around 100 nm was deposited on ITO coated PET by e-spray technique at the voltage of 3.7 kV with flow rate of 600 µl/hr using metal nozzle of internal diameter of 110 µm. The brief detail of PEDOT: PSS deposition can be found elsewhere [N. Duraisamy et. al.; 2012]. The resultant sample was subsequently cured at 100ºC for 30 minutes. After that, the deposition of the active polymer layer F8BT, was performed on top of the annealed PEDOT:PSS layer in the way mentioned above. Finally a 100nm thick Aluminium electrode was deposited on the active film by thermal evaporation at base pressures of ~$1x10^{-6}$ torr, concluding an active area of 3.15 mm^2 of the organic diode device.

2.2.1.1 Ink Characterization and Electrostatic Atomization

The identification of an operating envelope with a particular nozzle is mandatory for the ink characterization for electrostatic spray deposition process in order to have control on tailoring of the film properties like thickness etc. The experiment was first performed with varying flow rate from 300 µl/hr to 1000 µl/hr in order to determine optimum atomization envelope of the ink. At each flow rate, the different voltages were applied via high voltage DC source and their effect on ink droplet was observed. At different voltages, various modes of electro-hydrodynamic phenomena were recorded such as dripping, micro-dripping, unstable cone jet, stable cone jet known as Taylor Cone [H. F. Poon et. al] and multi-jet mode. Figure 2-8 provide the observed optimum operating envelope of the F8BT ink representing various atomization modes and Fig. 2-9 shows the high speed images of the e-spray atomization process events witnessed at different voltages keeping the flow rate

constant at 600 µl/hr. It was observed that at the flow rate of 600 µl/hr, without any voltage applied, only ink was dripping from the nozzle of a certain volume. As the voltage was gradually raised from zero, the droplets started detaching from the nozzle and at voltage of 3.4 kV, micro dripping was observed. With further increase in the voltage, a pulsating cone jet was observed at 3.5 kV emitting a long filament from the ink meniscus for instance. Then at a voltage 3.9 kV a stable single cone jet was witnessed. A few distances below the cone jet base, the jet broke up into a brush of drops. After raising the voltage further, two or more jets (multi-jetting) were observed at around 5.5 kV. If the applied voltage was further increased, the jet got discharged. A flow rate of 400 µl/hr has been selected for the fabrication of thin film of F8BT. This value is selected as the droplet has direct dependence on the flow rate. However if the flow rate is too low, the stable cone jet formation is going to be unstable after sufficient time span [A. Khan et. al.; 2011].

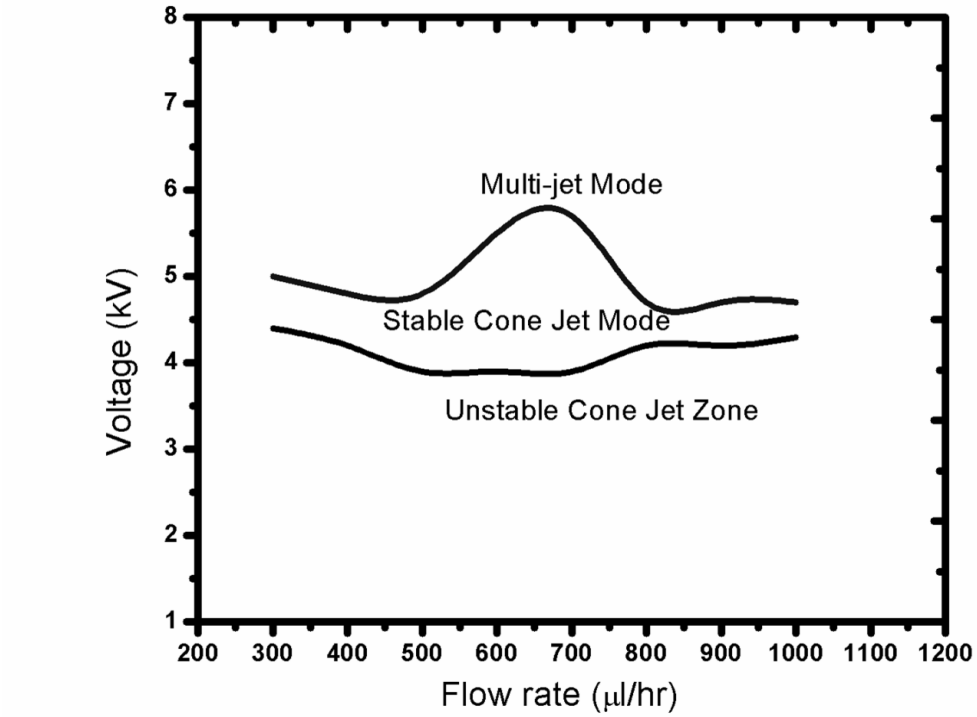

Figure 2-8: Operating envelope of the F8BT polymer ink.

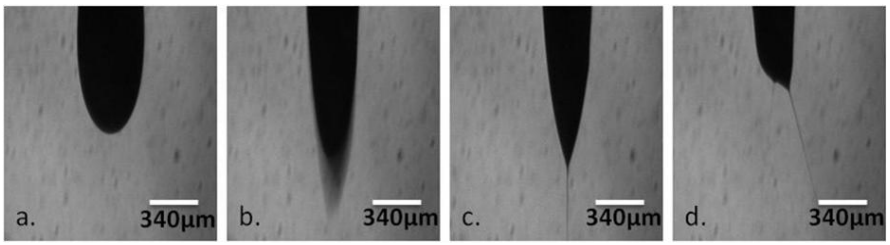

Figure 2-9: E-spray Atomization modes; a. Dripping mode, b. Unstable Cone jet mode, c. Stable Cone Jet mode, d. Multi-Cone Jet mode.

2.2.2 Thin Film Characterization

2.2.2.1 Structural Analysis

The fabrication of thin films of F8BT polymer on glass substrate was achieved at three different standoff distances followed by the annealing at the temperature of 100 °C for 30 min. The surface morphology of resultant samples were analyzed and compared. Field emission scanning electron microscope (FE-SEM) (JEOL JSM-7600F) was used to observe the surface morphology and the thickness of the

fabricated films. The quality of the film is highly dependent on the stand-off distance. Figure 2-10a, 2-10b and 2-10c show the images of surface morphologies of e-sprayed F8BT films deposited with nozzle-substrate distances of 19 mm, 20 mm and 21 mm respectively using a deposition speed of 3 mm/sec and making a single deposition pass. It was evident from morphological analysis that when the distance was 19 mm, most droplets landed on the substrate with incompletely evaporated solvent. This might be thought to form a wet as-deposit F8BT film, which results in the generation of spot thick layer causing uneven layer. At a distance of 20 mm, the unevenness of surface in the film disappeared and the film formed from polymer particles shows good morphology. As the distance become larger to 21 mm, the quantity of particles was reduced due to the reason that the droplets during spray spreading in all directions had covered larger area, and the prominent pores in the film started appearing. Therefore, it was concluded from this result that a standoff distance of 20 mm is the optimum for fabricating defect free F8BT film.

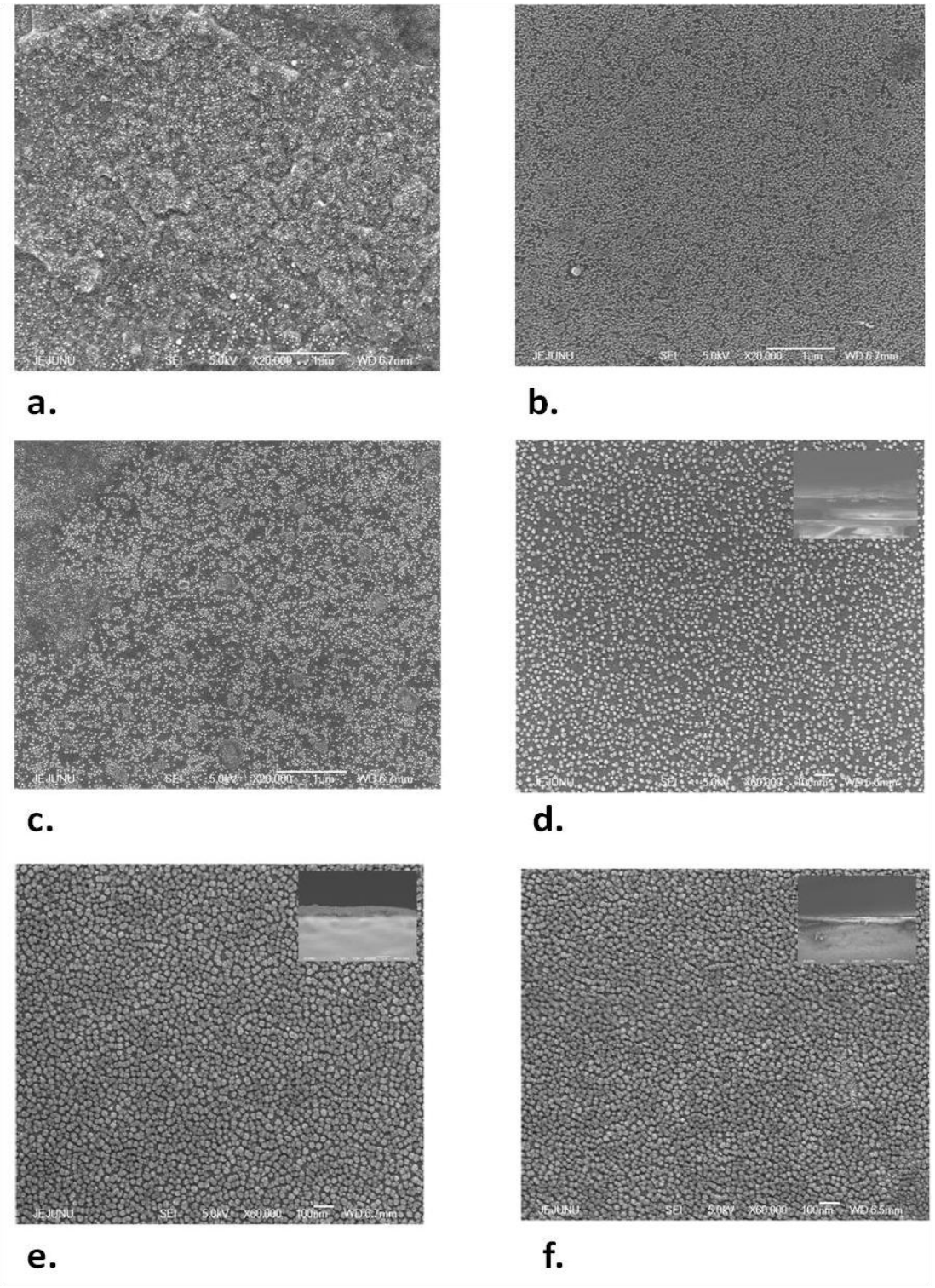

Figure 2-10: SEM image of F8BT film fabricated with the stand-off distance of: a. 19, b. 20 and c. 21 mm, and SEM image of F8BT film fabricated with; (d) single deposition pass, (e) two deposition pass, (f) three deposition pass; the inset shows the corresponding thickness of the film.

With the optimum distance of 20 mm, the effect of number of deposition passes on film quality was studied. Figure 2-10d, 2-10e and 2-10f show the SEM images of F8BT films deposited with nozzle-substrate distances of 20mm. With single pass, the less dense film was observed. With second pass, the film morphology was improved containing large number of particles. As the third pass of deposition was made, the much denser layer was witnessed. The insets of Fig. 2-10d, 2-10e and 2-10f shows the observed average thickness of 620 nm, 810 nm and 920 nm of F8BT films on glass substrates produced with one, two and three deposition pass respectively.

2.2.2.2 XPS Analysis

To investigate the surface composition of the film, X-ray Photoelectron spectroscopy (XPS) of the film was conducted using XPS analysis equipment (VG ESCA 2000, VG Microtech, England) equipped with a monochromated X-ray source. The XPS measurement was performed with pass energy of 100 eV and step size of 1 eV. Base pressure during the XPS analysis was kept at 1×10^{-7} Pa. Figure 2-11 shows the XPS spectra of the deposited F8BT thin film on glass obtained. The graph exhibits the peaks that were ascribed to S, N, C and O elements[A. L. Shu et. al.; 2012, M. K. Fung et. al.; 2003]

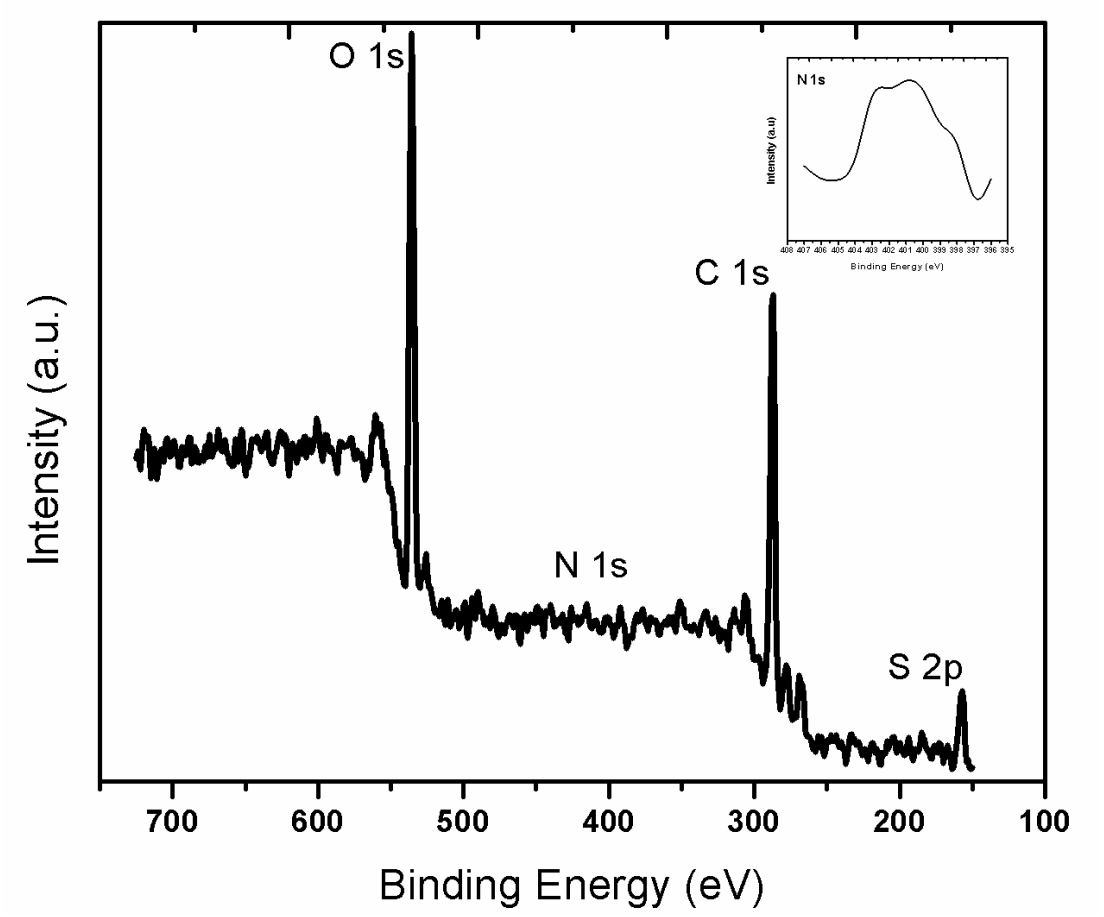

Figure 2-11: Wide-scan XPS spectra of the e-sprayed deposited F8BT thin film; Inset shows the close up scan of the N 1s peak.

2.2.2.3 Optical Analysis

The optical studies of e-sprayed F8BT film on glass were done by using a Ultra-violet/Visible spectrometer (Shimadzu UV-3150) in order to record UV-Visible (UV-Vis) data with range of 350-800 nm. Absorbance in the UV-Vis region measures the transitions from the ground state to the excited state at specific wavelength which is attributed to the material nature. UV–Vis absorption spectra of F8BT films for each number of deposition passes are shown in Fig. 2-12. The UV-Vis plot of the deposited film does compare favorably to that found in literature [T. Fukuda et. al.; 2009, R. K. Gupta et. al.; 2008, F. Dou et. al.; 2011]. Each absorption spectrum of F8BT film was peaked at about 462 nm. There is almost no shift of the

peak located at wavelength of 462 nm with each number of passes. An increase in intensity was observed with each number of deposition passes that indicates that more dense film was achieved with each number of pass which accords with SEM analysis too. Overall the result suggests that the thin film shows good optical properties.

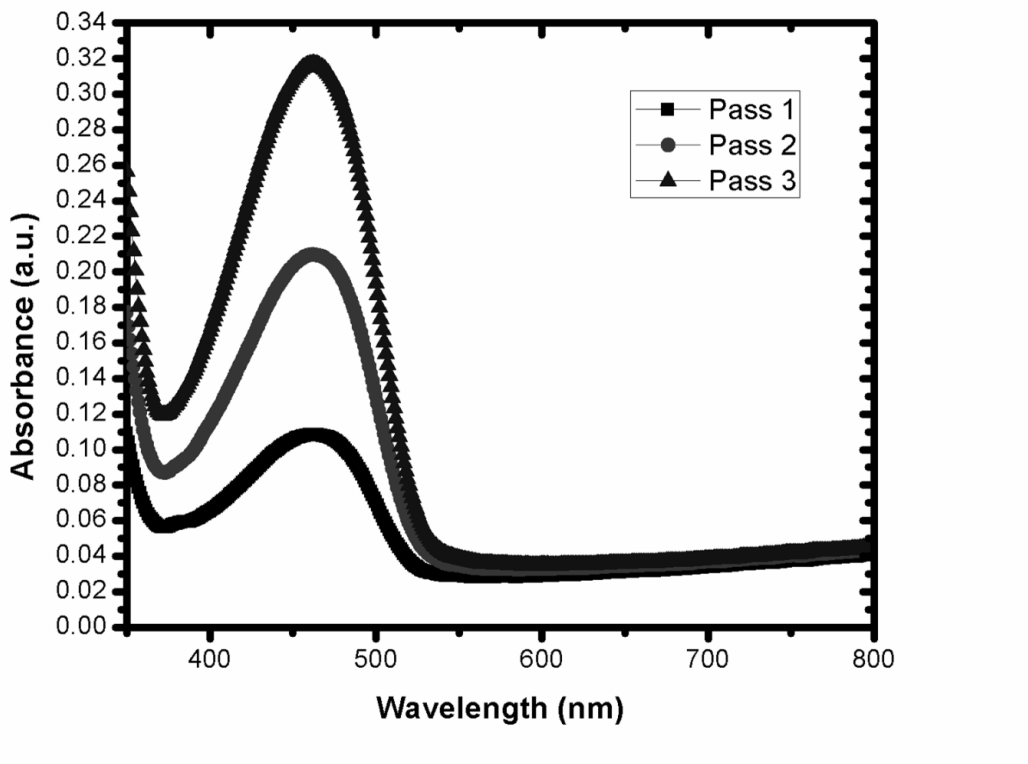

Figure 2-12: Absorbance spectra of F8BT thin film for three different number of deposition passes.

2.2.2.4 IV Analysis

After the optimization of parameters of e-spray process, an organic diode with a structure of ITO/PEDOT:PSS/F8BT/Al was fabricated having e-sprayed F8BT film as an active semiconducting layer of thickness of ~810nm. The schematic picture of organic diode device with structure configuration ITO/PEDOT:PSS/F8BT/Al is depicted in Fig. 2-13. The feasibility of e-spray technique for the multi-layered structured diode was analyzed by performing current-voltage measurement using semiconductor analyzer (Agilent B1500A).

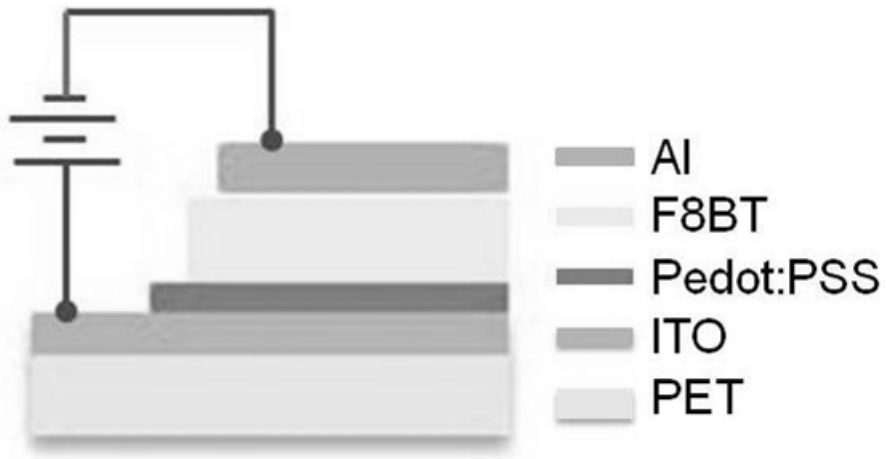

Figure 2-13: The pictorial picture of the ITO/PEDOT:PSS/F8BT/Al organic diode device.

Electrical behavior of the multi-layer films in electronic devices is very much dependent on the proper adhesion of the two adjacent films for its satisfactory performance. The current density-voltage (JV) curve of the organic diode structures in linear scale recorded by semiconductor analyzer was shown in Fig. 2.14a. By the JV plot, it is evident that there is proper contact between each adjacent layer. At voltage of 1.38 V, the current density in organic structure is at low value of 6.55×10^{-6} A/mm^2 and after that as further voltage was applied, the device current density increased by the order of 10 and reaches upto 6.54×10^{-5} A/mm^2 at voltage of 2.5 V indicating an increase in charge carrier injection. The JV characteristic semilograthimic plot as shown in Fig. 2.14b reveals a non-ideal current-voltage behavior of the device and confirms the formation of the ITO/PEDOT-PSS/F8BT interface.

In a diode, when the higher carrier densities from one electrical contact are locally injected into material, the space charge limited currents may take place and can be identified by analyzing the behavior of curve of JV in log-log scale [R. K Gupta et. al.; 2004]. The plot of logJ vs logV was made as shown in Fig. 10 and was

analyzed using $J = bV^{m}$ relationship [A. A Gringer et. al.; 1989] where "m" represents the slope. The dominant charge transport mechanism for the diode was determined by obtaining "m" values from the slopes of linear regions in Fig. 2.14c.

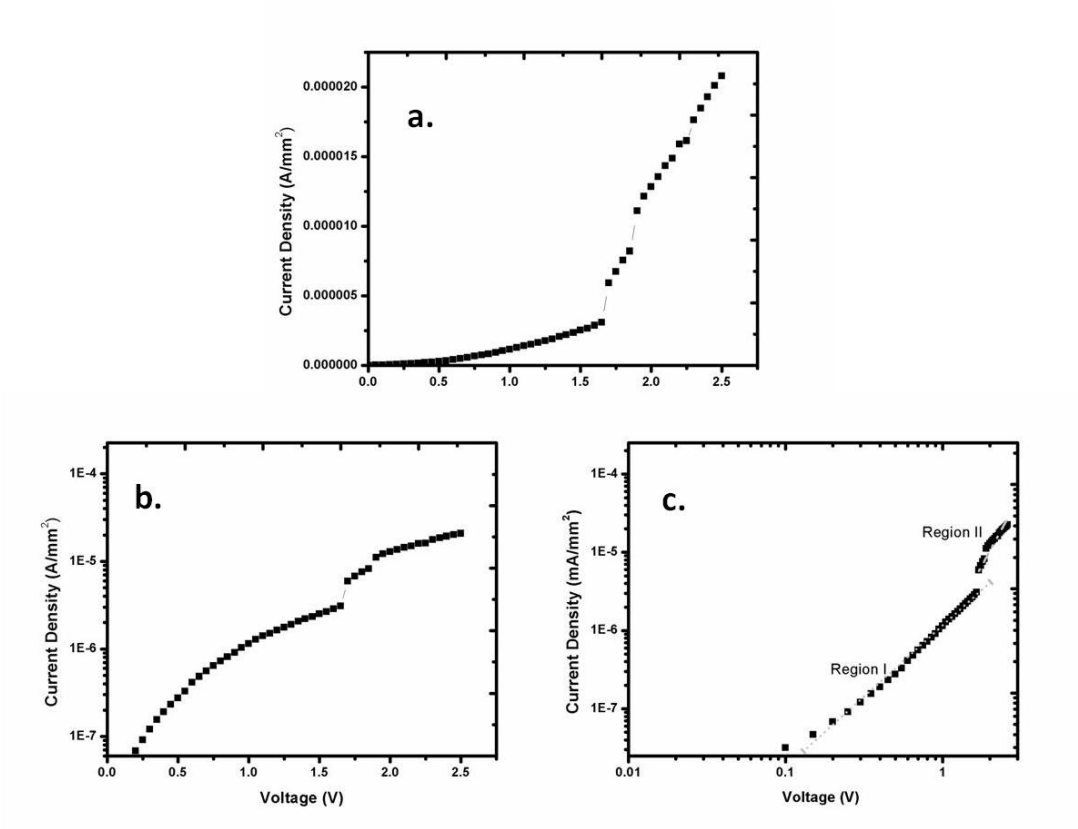

Figure 2-14: JV plot of the ITO/PEDOT:PSS/F8BT/Al organic diode having e-spray deposited F8BT thin film; a. in linear scale, b. in semilograthimic scale, c. in Log-Log scale.

The slope of the first and second region shown in Fig. 3-7c was found to be 1.968 and 1.945 respectively close to 2, indicating the presence of space charge limited conduction [R. K Gupta et. al.; 2004] . For an organic semiconductor with the space charge limited conduction, the mobility was determined from the well known equation of the space charge limited current model [A. A Gringer et. al.; 1989] and was found to be $5.65e^{-4}$ cm^2 $V^{-1}s^{-1}$ that appears to be reasonable for organic semiconductors [Y. Zhang et. al.; 2011, A. R. Inigo et. al.; 2003].

2.2.3 Conclusions

Fabrication of conjugated polymer F8BT thin film has been achieved using a cost effective vacuum-free electrostatic spray technique. The dependence of morphology of polymer films on the parametric standoff distance was observed. The deposition thickness was controlled by number of deposition passes. The elemental composition of the film was confirmed through the XPS analysis. The e-spray deposited F8BT films for each number of deposition passes showed the absorption edge at wavelength of 462 nm. The performance of fabricated organic diode with F8BT film deposited by e-spray techniques was satisfactory. Contact between the two adjacent polymers layers in organic diode structure with e-spray deposited F8BT film was proper as evident from the JV characteristic curve of the organic diodes. With the e-spray FEBT film, the organic diode device showed carrier mobility value of $5.65e^{-4}$ cm^2 $V^{-1}s^{-1}$. OLED devices with thin F8BT emissive layer show good current transporting properties and electroluminescence performance because of proper contact between the adjacent layers in organic diode structure. The structural, optical and electrical results achieved by this study have enlighten e-spray technique as an promising method for the next generation printed nano-electronic devices and can also be explored to fabricate low-cost optoelectronic devices.

2.3 2,9-dimethyl-4,7-diphenyl-1,10-phenanthroline Organic Thin Film

During the past decade, small-molecule (SM) based organic semiconducting thin films have gained much attentions in relation to their possible applications to the next generation organic electronics such as organic thin film transistor [Jr. Demchuk et. al; 1995, D. J.Gundlach et. al.; 1997] and optoelectronics devices [M. Shtein et. al.;

2002, K. M. Vaeth et. al; 2003, R. U. A. Khan et. al.; 2006, P. Peumans et. al.; 2001, P. Peumans et. al.; 2003, S. R. Forrest et. al.; 2004]. Vacuum-based deposition processes such as thermal evaporation technique under high vacuum etc are generally used to fabricate high-quality thin films of SM organic thin films [S. R. Forrest et. al.; 2004, G. Gu et. al.; 1997]. However, these processes increase the fabrication complexity with high loss of the expensive organic materials. Additionally, the use of evaporation masks would limit the scalability and resolution architecture of large-area organic microelectronic devices. Spin coating is another method used to apply uniform organic thin films to flat substrates in which an excess amount of an ink is applied to a rotating substrate. But for larger substrate, the throughput of the spin coating process decreases. Hence, there is a need of adopting a film fabrication technology to fabricate high-quality films for implementation in electronic applications in cost-effective fashion and also capable to handle large-scale production.

Electrospray deposition (ESD) is a recently developed vacuum-free technique to fabricate the wide variety of thin films of functional materials which are used in large area semiconductor electronic device applications [A. Van Zomeren et. al.; 1994, P. Miao et al; 2001, D. H. Youn et. al.; 2009, A. Gupta et. al.; 2007, R. Bakhshi et. al.; 2009, A. khan et. al.; 2001, M. Mustafa et. al.; 2012, N. Duraisamy et. al.; 2012]. The primary advantage of this technique is that with the simple experimental setup without special vacuum conditions, it has the ability to fabricate multilayer architecture of thin films with high uniformity and good morphology with large area coverage without damaging the underlying organic layer [I. Hayati et. al.; 1986, H. F. Poon et. al.; 2002]. This method involves the atomization of ink

containing functional material through very fine spray nozzle with the application of electric field over the entire substrate under stable cone-jet spray mode condition, there by depositing a thin film of functional material on it. The complete details of ESD process can be found elsewhere [I. Hayati et. al.; 1986, H. F. Poon et. al.; 2002, K. H. Choi et. al.; 2012] .

In this section, the fabrication of SM based organic thin film by ESD technique has been demonstrated. Bathocuproine also known as 2,9-dimethyl-4,7-diphenyl-1,10-phenanthroline (BCP) was selected as a small organic material. It is the wide-band gap material, n-type semiconductor materials extensively used as buffer layer for optoelectronic devices [P. Peumans et.al.; 2000, H. Xin et.al.; 2003, H. Gommans et. al.; 2008]. BCP ink was synthesized in-house and was subjected to electrostatic atomization under the influence of applied electric field. The operating parametric envelope of the BCP ink was recorded. After that, the thin film fabrication was carried out on glass substrates followed by thermal annealing of the film. The surface morphology of the resultant films was investigated in order to observe the film quality. The elemental composition of the BCP film was confirmed by X-ray Photoelectron spectroscopy (XPS) analysis and then optical characterization was carried out at room temperature. For electrical performance analysis, the attempt was made to fabricate a prototype multi-layer organic diode device having ESD deposited BCP thin film as a buffer layer. The performance of organic diode device was analyzed by performing current-voltage measurement.

2.3.1 Small Molecule based BCP Organic Thin Film Deposition

Materials

The BCP polymer powder (Avg. Mol wt: 384.5), F8BT powder (Avg. Mol wt: 10,000-20,000) and ITO coated PET substrate were purchased from Sigma Aldrich, South Korea. The PEDOT:PSS (Orgacon) was supplied by Agfa Materials Japan Limited, Japan. The tetrahydrofuran, acetone and ethanol solvents were purchased from Daejon Chemical and Metal Co. Ltd, South Korea.

Ink Preparation and Experimental Setup

As a first step, the BCP ink was made by dissolving BCP powder in ethanol solvent at a content of 0.1g/ml at room temperature. The resultant solution was bath-sonicated for 30 min at room temperature and was then used for ESD process. The in-house built ESD system is consist of the stainless steel metal nozzle (O.D 340µm) attached to nozzle adapter (nozzle holder) mounted over the substrate which was placed on flat movable stage whose motion is controllable by the computer. The ink was placed in a 1-ml glass syringe mounted in the syringe pump (Harvard Apparatus, PHD 2000 Infusion) and was supplied to the nozzle through silicon tubing. The anode of high voltage source was connected to metallic nozzle and the ground was given to the movable stage. A high resolution CCD camera (Motion Pro X) connected to the computer along with a light source was used to visualize and record the ink flow under electric field. The distance of 5 mm was maintained between the nozzle and substrate. For continuous film fabrication, the speed of the moving stage was set at 3 mm/sec. The operating envelope for ink was obtained by using the combination of voltage and flow rate. The flow rate was raised from 40 µl/hr to 200 µl/hr and the voltage was gradually increased from 0 kV to upto 3.5 kV in order to

observe different operating modes of functional spray. A schematic of the experimental arrangement of ESD system is shown in Fig. 1-7.

Film Fabrication

For thin film fabrication, the glass substrate was cleaned with acetone for 15 min followed by rinsing with deionized water and finally dried at room temperature and was placed on the movable stage. After that, BCP thin film samples were prepared by depositing of BCP layer on to a glass with the flow rate of 100 µl/hr under the condition of stable cone jet mode. The number of deposition passes was varied in order to fabricate thin films of different thicknesses. The resultant samples were sintered at 60 ºC for 30 min and were then characterized by using different thin film characterization tools.

In order to evaluate the electrical performance of electrosprayed BCP film, the prototype multi-layer organic diode device was fabricated as follow: firstly the ITO coated PET substrate was cleaned and was further treated with oxygen plasma for 1 min followed by the deposition of PEDOT:PSS as hole injection layer. For that, a layer of PEDOT:PSS with thickness of around 100 nm was deposited on ITO coated PET by spin coating technique with 1500 rpm for 30 sec. The resultant sample was subsequently cured at 100 ºC for 30 min. The deposition of the active polymer layer F8BT of around 125 nm thickness, was made on top of the cured PEDOT:PSS layer with an ink composed of 1.1 gm per ml of tetrahydrofuran via spin coating technique followed by annealing at 100ºC for 30 minutes. BCP layer was deposited on top of the annealed F8BT layer in the same way mentioned above. Finally a 100 nm thick aluminum electrode was deposited on the active film by thermal evaporation at base

pressures of ~1x10^{-6} torr. The active area of the device, defined by the overlap of the ITO and Al electrode, was about 0.0315 cm^2.

Characterization techniques

The surface morphology inspection of the fabricated BCP films was performed by using Field Emission Scanning Electron Microscope (FE-SEM) (JEOL JSM-7600F, Japan) machine operated at the accelerating voltage of 5 kV. For film thickness measurement, non-destructive thin film thickness machine K-MAC ST4000-DLX was used. To look into elemental composition of the film, X-ray Photoelectron spectroscopy (XPS) of the film was conducted using XPS analysis equipment (VG ESCA 2000, VG Microtech, England) equipped with a monochromated X-ray source. Base pressure during the XPS analysis was kept at 1 × 10-9 Pa. The optical analysis of ESD deposited BCP film on glass were done by using a Ultra-violet/Visible spectrometer (Shimadzu UV-3150) in order to record UV-Visible (UV-Vis) data within range of 200-800 nm. For electrical characterization, the Agilent B1500A Semiconductor Device Analyzer coupled with MST8000C Probe Station having a current resolution of 1fA was used.

2.3.1.1 Ink Characterization and Spray Formation

To have a control on tailoring of the film properties like thickness etc, the identification of an operating envelope with a particular nozzle is mandatory for the ink characterization for electrospray deposition process. In order to determine optimum atomization envelope of the ink, the experiment was performed with varying flow rate from 40 µl/hr to 200 µl/hr and at each flow rate, the different voltages were applied via high voltage DC source. At different voltages keeping flow rate constant, various electro-hydrodynamic spray modes were recorded such as dripping, micro-dripping, unstable cone jet, stable cone jet known as Taylor Cone [

H. F. Poon et. al.; 2002] and multi-jet mode. Figure 2-15 provides the observed optimum operating envelope of the BCP ink representing various electro-hydrodynamic phenomena zones and Fig. 2-16 shows the high speed images of the spray functional modes witnessed at different voltages keeping the flow rate constant at 80 µl/hr. It was observed that at the flow rate of 80 µl/hr, dripping mode of spray was observed when no voltage was applied. As the voltage was gradually raised from zero, the droplets started detaching from the nozzle and at voltage of 1.9 kV, micro-dripping was observed. With further increase in the voltage, a pulsating cone jet mode was observed at 2.1 kV and the pulsation frequency of the jet increased with increasing voltage. At critical voltage value of 2.5 kV, a stable single cone jet was witnessed. A few distances below the cone jet base, the jet broke up into a brush of drops. After raising the voltage further, tip of the jet becomes unstable and two or more jets (multi-jetting) appeared at around 3.1 kV. If the applied voltage was further increased, the jet got discharged. A flow rate of 100 µl/hr has been selected for the fabrication of thin film of BCP. This value is selected as the droplet has direct dependence on the flow rate. However if the flow rate is too low, the stable cone jet formation is going to be unstable after sufficient time span [H. F. Poon et. al.; 2002].

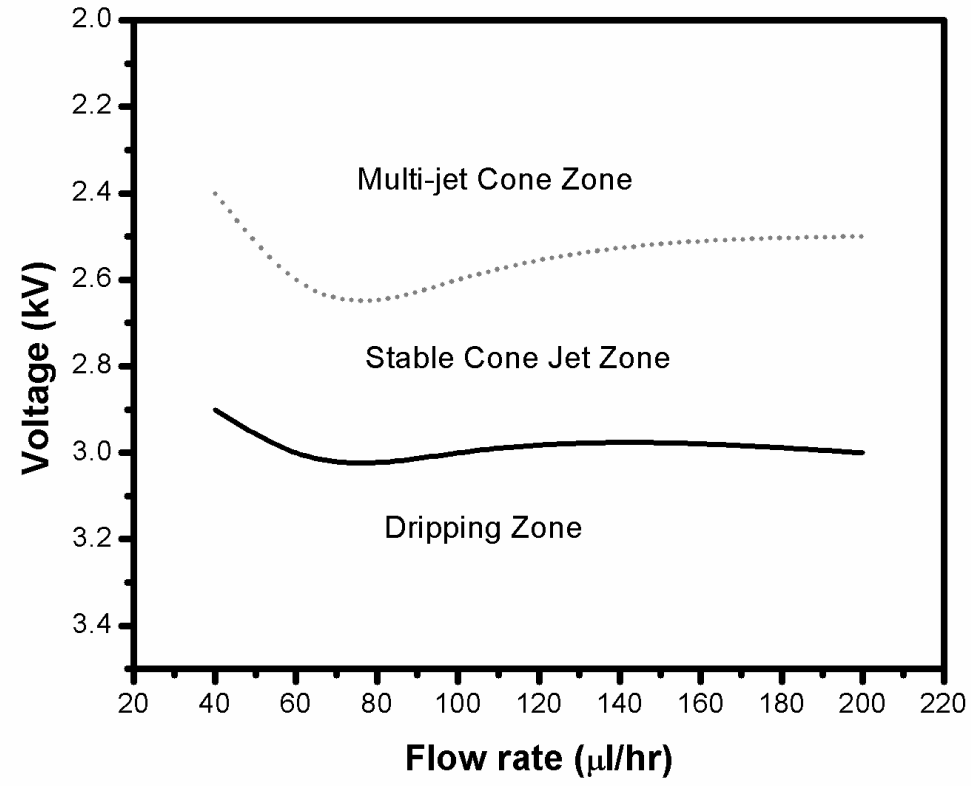

Figure 2-15: Operating envelope of the BCP organic ink.
Figure 2:

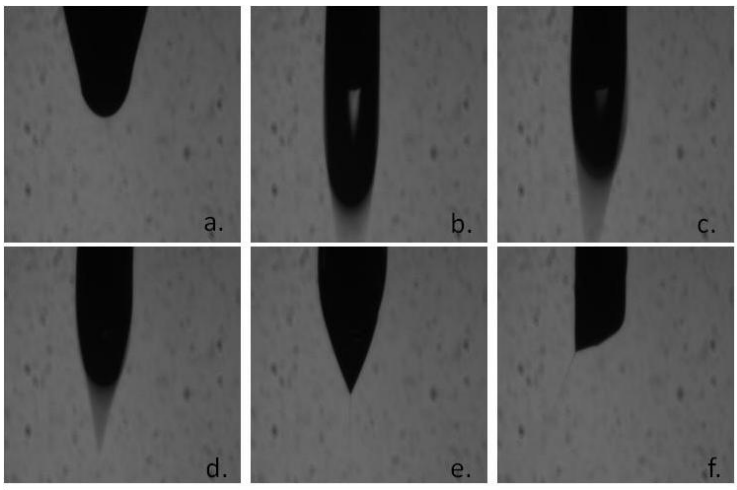

Figure 2-16: Functional spray modes; a. Dripping mode, b. Micro-dripping, c. Unstable Cone jet mode, d. Highly Pulsating Cone jet mode, e. Stable Cone Jet mode, f. Multi-Cone Jet mode.

2.3.2 Thin Film Characterization

2.3.2.1 Structural Analysis

The fabrication of BCP thin film on glass substrate was achieved with nozzle-substrate distances of 5 mm using a deposition speed of 3 mm/sec and making a single deposition pass followed by the annealing at the temperature of 60 °C for 30 min. The detail surface morphology of the prepared sample films was observed by carrying out FE-SEM analysis. Figure 2-17 shows a high magnification FE-SEM image representing the surface morphology of BCP film on bare glass. As clear from the SEM image, the densely packed layer was observed without any prominent pores, thereby implying that fabricated SM based organic thin film using ESD technique is suitable for electrical and optical applications.

Variation in film thickness as a function of ESD deposition passes given has been studied. The thicknesses of the BCP films achieved with different number of passes were recorded as shown in Fig. 2-18. The minimum thickness achieved by the ESD deposition technique is 75nm ± 20nm which is compatible with high quality vacuum based BCP film demonstrated elsewhere [W. Stampor et. al.; 2011]. The maximum thickness achieved is 88nm ± 20nm by four deposition passes.

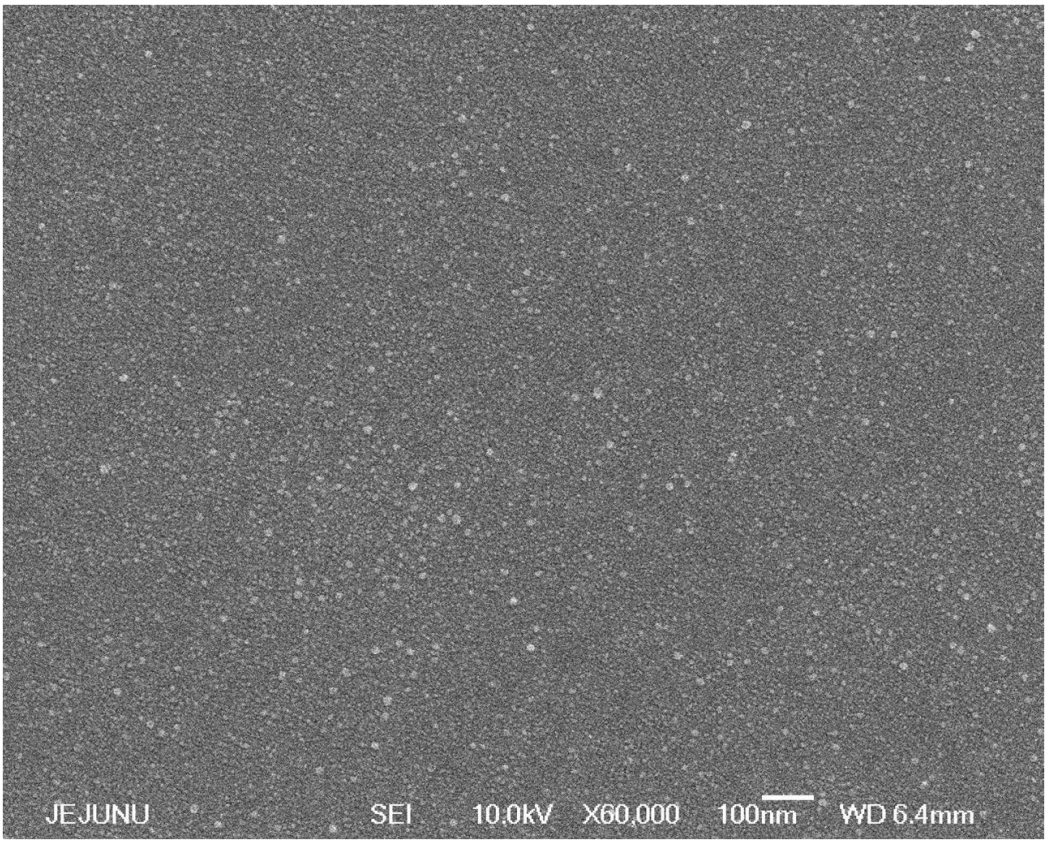

Figure 2-17: SEM image of BCP film fabricated at the stand-off distance of 5 mm with the single-step deposition pass.

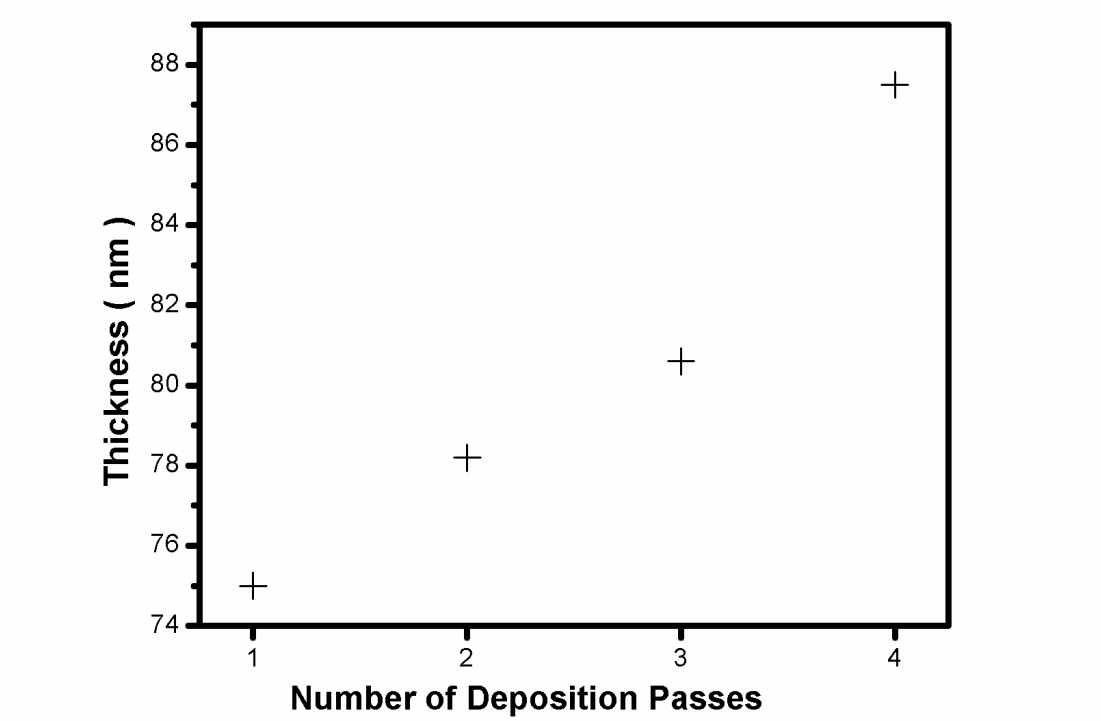

Figure 2-18: Variation of the thin film of electrosprayed BCP with number of ESD deposition passes with moving substrate speed of 3mm/sec.

2.3.2.2 XPS Analysis

Figure 2-19 shows the XPS spectrum of the deposited BCP thin film on glass. The spectrum exhibits the prominent peaks that were ascribed to C (284.51 eV) and O (531.74 eV) elements [J. H. Seo et. al.; 2007, S. Huang et. al.; 2011] [27, 28]. The inset of Fig. 2-19 shows the narrow scan highlighting the presence of N (398.27) element.

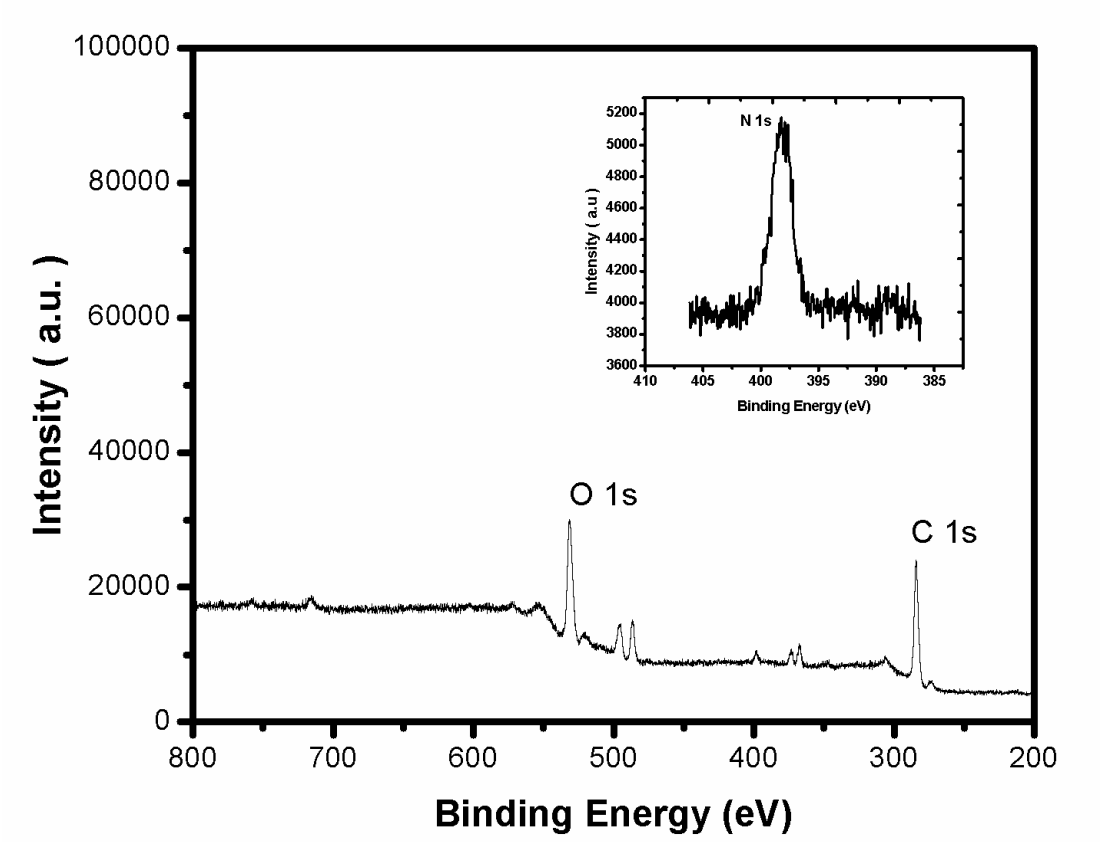

Figure 2-19: Wide-scan XPS spectra of the e-sprayed deposited F8BT thin film; Inset shows the narrow- scan XPS spectra indicating N 1s peak.

2.3.2.3 Optical Analysis

The plot UV–Vis absorption graph of BCP films for each number of deposition passes verse wavelength are shown in Fig. 2-20. It is clearly shows that there is nearly no absorption in the range of visible light. Each absorption spectrum of BCP film was peaked at about 286 nm. There is almost no shift of the peak located at wavelength of 286 nm with each number of passes. The UV-Vis plot of the deposited

film does compare favorably to that found in literature [W. Stampor et. al.; 2011, Z. T. Liu et. al.; 2005]. A slight increase in intensity was observed with each number of deposition passes that indicates that denser film was achieved with each number of pass which accords with thickness analysis too. In order to determine the optical band gap of the BCP thin film, the absorption coefficient α for the films was calculated using the relation $\alpha = 2.303\ A/t$ where, A is the absorbance of the film and t its thickness. The square of absorption coefficient and photons energy $(\alpha\ hv)^2$ was calculated and was related to the energy gap and photon energy hv according to the Tauc's relation [S. Varghese et. al.; 2002]. From the graph of $(\alpha hv)^2$ verses photon energy shown in the inset of Fig. 4-6, the energy gap for the electrosprayed BCP film was determined by extrapolating the linear part of the curve equals to 0 and was found to be 3.5 eV which accords with value found in literature [Q. L. Song et. al.; 2005, P. Peumans et. al.; 2001].

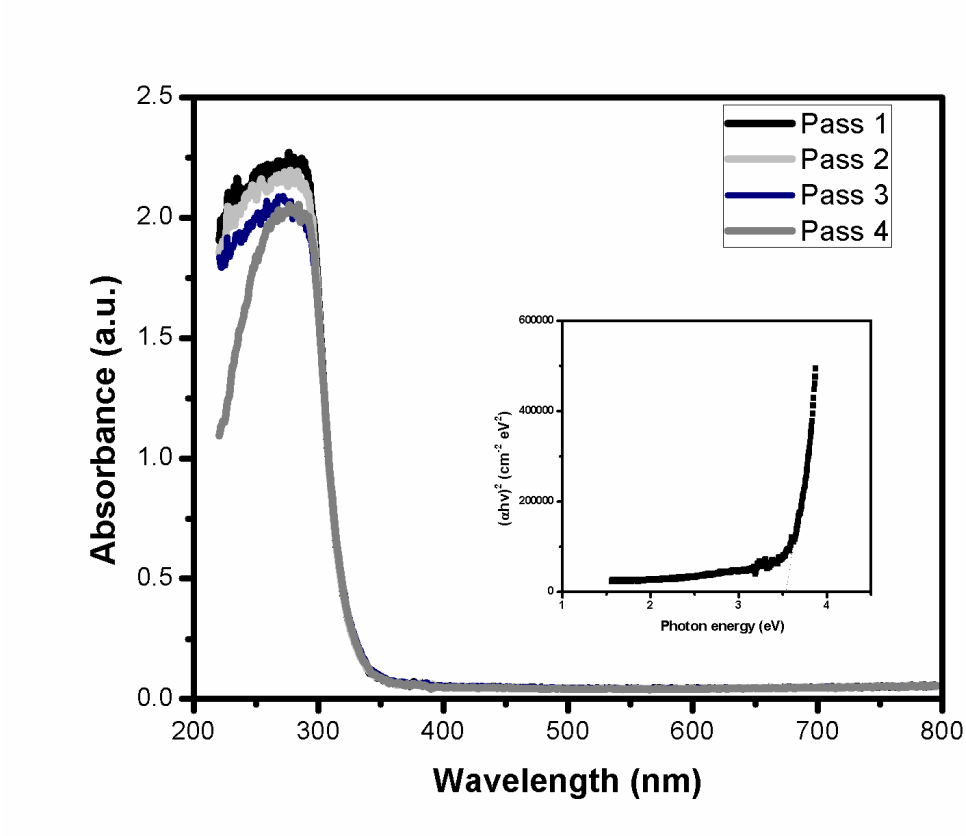

Figure 2-20: Absorbance spectrum of BCP thin film for four different number of deposition passes; the insets shows the plot of $(\alpha hv)^2$ verses photon energy for BCP thin film of 75 nm thickness.

2.3.3 Conclusions

Fabrication of SM based organic BCP thin film has been achieved using a cost effective, vacuum-free electrospray deposition technique. The film thickness was controlled by number of deposition passes. The elemental composition of the film was confirmed through the XPS analysis. The BCP films for each number of deposition passes showed the absorption edge at wavelength of 286 nm and the energy gap of the film was measured to be 3.5 eV. The electrical performance of fabricated prototype organic diode with BCP film deposited by ESD techniques was satisfactory. Contact between the two adjacent polymers layers in organic diode structure with electropray deposited BCP film was proper as evident from the increase in current density with voltage in J-V characteristic curve of the organic

diode. The structural, optical and electrical results achieved by this study have enlighten electrospray deposition technique as a promising method to develop small molecule based organic thin film for the next generation printed electronic devices and can also be further explored to fabricate low-cost optoelectronic devices .

3 Organic Light Emitting Devices Fabrication and Performance Evaluation using electrospray deposited Functional thin films

3.1 MEH-PPV Polymer based OLED

3.1.1 OLED Device Fabrication

In order to check the functionality of diode behavior having MEH-PPV layer, a bi-layer based electronic diode structure was developed. Firstly the cleaned flexible ITO coated PET as anode having pre-fabricated PEDOT:PSS layer on it was taken. Then the MEH-PPV ink was electrically atomized on the PEDOT:PSS layer in the same manner as mentioned before using evaluated optimized parameters of electrospray, cured at 100 ˚C for 5 hours and after then was electrically characterized. For comparison with spin coating deposition process, the same diode structure was developed by spin coating the same ink solution on the ITO coated PET having pre-fabricated PEDOT: PSS at 2000 rpm for 60 sec. Minolta LS-100 luminance meter was used to measure luminous intensity and to collect the Commission International d'Eclairage (CIE) coordinators (x,y) for the identification of color. The electroluminescence (EL) of devices was measured by calibarated spectrometer (Avantes AvaSpec-ULS2048 StarLine Versatile Fiber-optic). Figure 4-1shows the schematic picture for fabrication process of OLED device.

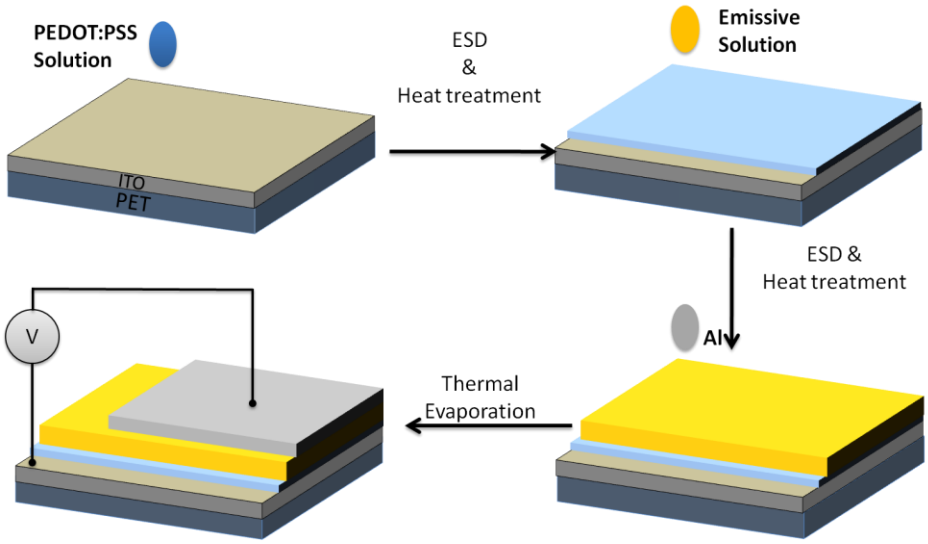

Figure 3-1: Schematic diagram illustration of the fabrication process for multi-layered MEH-PPV OLED device.

3.1.2 OLED Device Performance

Table 4-1 shows the driving voltage of the OLED device required to generate the maximum luminous intensity of 1 lux. The device gave luminous intensity of 1 lux at the operating voltages of 11 V. Orange red electroluminescence emission spectrum centered at ~ 585 nm was measured for the device when operated in continuous DC mode as shown in Fig. 4-2. The color coordinates in CIE chromaticity of OLED was (x,y = 0.56, 0.43), which lie in the orange red region as shown in Fig. 4-2 and accords with the electroluminescence results as well. An optical image of orange red light emission from the device was shown in the Fig. 4-3.

Table 3-1: The experimental values of luminous intensity of MEH-PPV based OLED devices.

EL Material	**Brightness (lux)**	**CIE (x,y)**	**Voltage (V)**
MEH-PPV	1	0.56,0.43	11

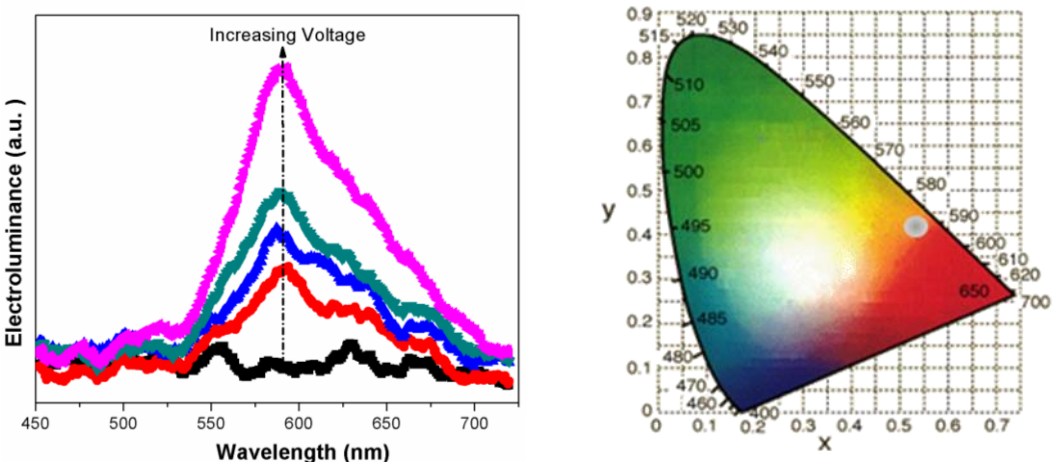

Figure 3-2: Electroluminance of the OLED device at on state (left side) and CIE coordinates for OLED device having electrosprayed MEH-PPV as an active layer.

Figure 3-3: Optical Image of the orange light emission from the MEH-PPV based device.

3.2 F8BT Polymer thin film based OLED

3.2.1 OLED Device Performance

For organic diode fabrication, the ITO coated PET substrate was cleaned and was oxygen plasma treated for 1 min. After that, the deposition of PEDOT:PSS as hole injection material was performed. For that, a layer of PEDOT:PSS of thickness of around 100 nm was deposited on ITO coated PET by e-spray technique at the voltage of 3.7 kV with flow rate of 600 µl/hr using metal nozzle of internal diameter of 110 µm. The brief detail of PEDOT: PSS deposition can be found elsewhere [N. Duraisamy et. al.; 2012]. The resultant sample was subsequently cured at 100ºC for 30 minutes. After that, the deposition of the active polymer layer F8BT, was performed on top of the annealed PEDOT:PSS layer in the way mentioned above.

Finally a 100nm thick Aluminium electrode was deposited on the active film by thermal evaporation at base pressures of ~1x10^{-6} torr, concluding an active area of 0.64 cm^2 of the organic diode device. The schematic picture is shown in Fig 4-4 and Figure 4-5 shows the schematic picture for fabrication process of OLED device.

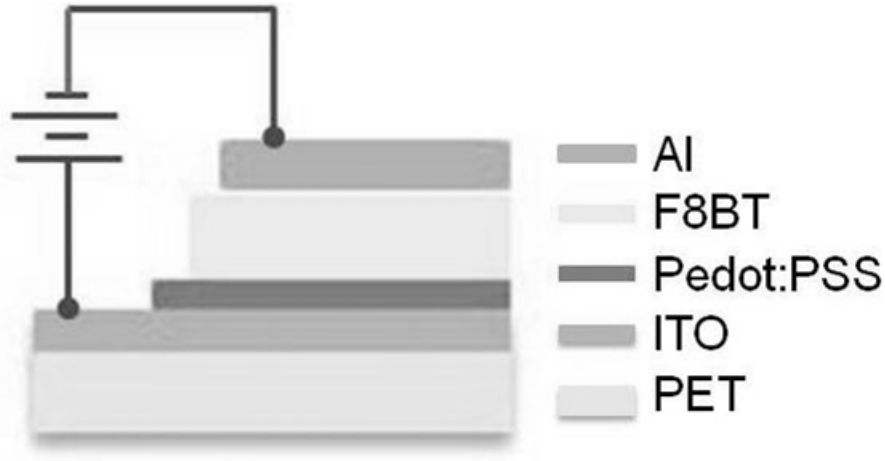

Figure 3-4: Schematic illustration of ITO/Pedot:PSS/F8BT/Al OLED device.

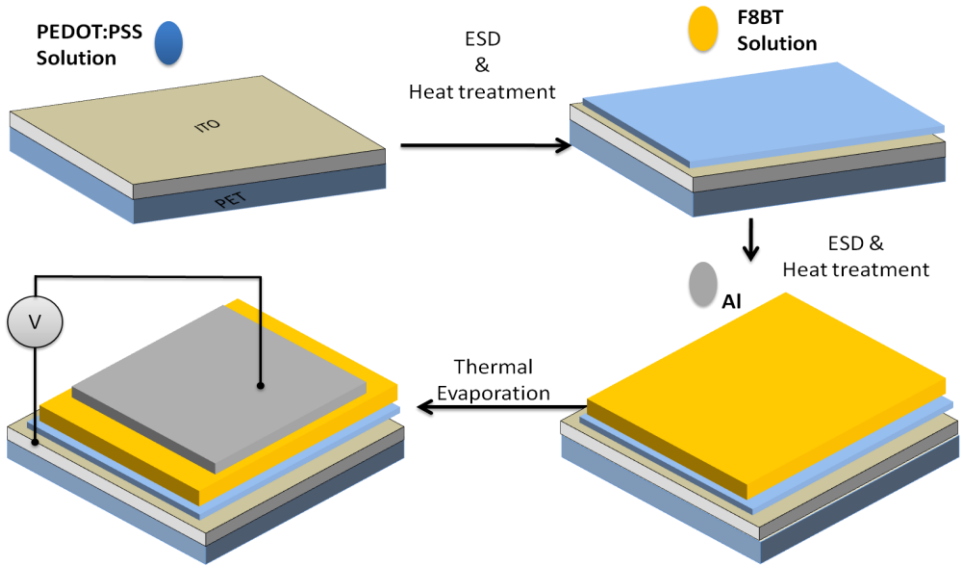

Figure 3-5: Schematic diagram illustration of the fabrication process for multi-layered F8BT OLED device.

3.2.2 OLED Device Performance

Table 4-2 shows the driving voltage of the OLED device required to generate the maximum luminous intensity of 0.3 lux. The device gave luminous intensity of 0.3 lux at the operating voltages of 8 V. Green electroluminescence emission spectrum centered at 545 nm was measured for the device when operated in continuous DC mode under forward bias as shown in Fig. 4-6. Figure 4-6 depicts EL spectra from this device collected at different voltages.. In these spectra, the peak at 545 nm is the characteristic emission bands of F8BT based device. The color coordinates in CIE chromaticity of OLED was (x,y = 0.46, 0.6), which lie in the pure green region as shown in Fig. 4-6 and accords with the electroluminescence results as well. An optical image of green light emission from the device was shown in the Fig. 4-7.

Table 3-2: The experimental values of luminous intensity of F8BT based OLED devices

EL Material	Brightness (lux)	CIE (x,y)	Voltage (V)
F8BT	0.3	0.4,0.6	8.4

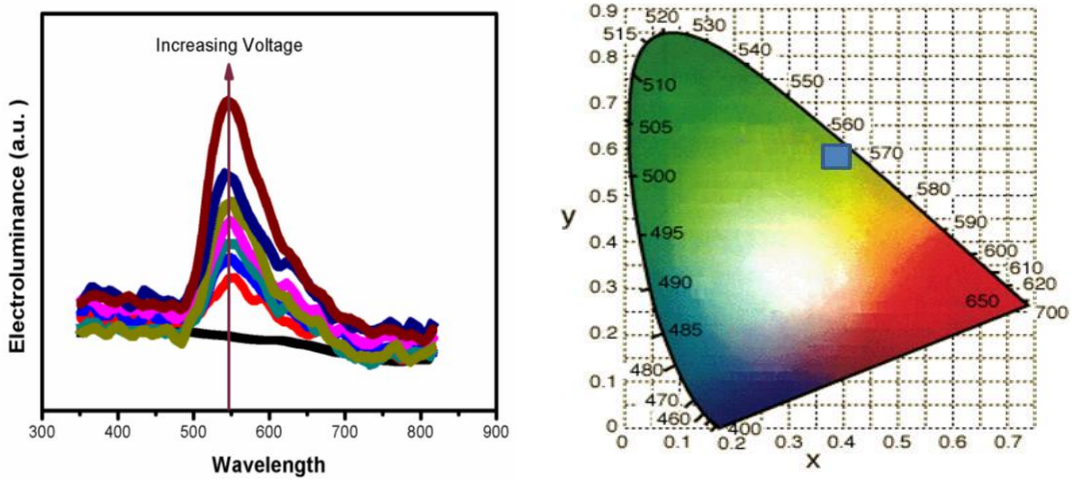

Figure 3-6: Electroluminance of the OLED device under forward bais (left side) and CIE coordinates for OLED device having electrosprayed F8BT as an active layer.

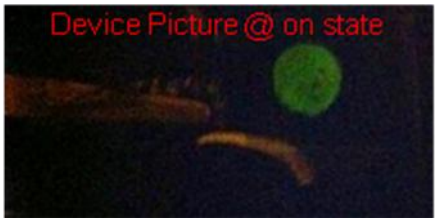

Figure 3-7: Optical Image of the orange light emission from the F8BT based device.

3.3 F8BT Polymer thin film based OLED with BCP as EIL

3.3.1 OLED Device Preparation

In order to verify the electrical performance of BCP film, a prototype multi-layer organic diode device with a structure of ITO/PEDOT:PSS/F8BT/BCP/Al was fabricated having electrosprayed BCP film as a buffer layer of thickness of ~80nm. The active area of the device is 0.64 cm^2. The schematic picture of organic diode device with structure configuration ITO/PEDOT:PSS/F8BT/BCP/Al is shown in Fig. 4-8. Figure 4-9 shows the schematic picture for fabrication process of OLED device.

3.3.2 OLED Device Performance

The current density-voltage (J-V) characteristics curve of the organic diode structures in linear scale was shown in Fig. 4-10 recorded by semiconductor analyzer. The inset shows the J-V characteristic semilograthimic plot which reveals a non-ideal current-voltage behavior of the device and confirms the formation of the ITO/PEDOT-PSS/F8BT/BCP interface. At voltage of 1 V, the current density in device was at low value of 8.4×10^{-6} A/cm^2 and as further voltage was applied, the device current density increased by the order of 10^2 and reaches upto 2×10^{-4} A/cm^2 at an operating voltage of 2.5 V indicating an increase in charge carrier injection. In a diode, the behavior of characteristics curve of J-V in log-log scale identify the

current conduction mechanisms for the diode device and can be analyzed using $J = bV^m$ relationship [A. A. Gringer et. al.; 1989] where "m" represents the slope. The dominant charge transport mechanism for the diode was determined by obtaining "m" values from the slopes of linear regions in Fig. 4-11. The curve can be divided into three region having three different slopes. The slope of the first, region is 1 as shown in Fig. 4-9, indicating the presence of ohmic region where the current density is directly proportional to operating voltage. The slopes of second region and third region were found to be 2 and 3.4 at higher values of voltage respectively indicating the presence of space charge limited conduction and trap charged current limited mechanism respectively that could be related to the filling of trap sites of semiconducting organic layers by injected carriers [Y. Zhang et. al.; 2011].

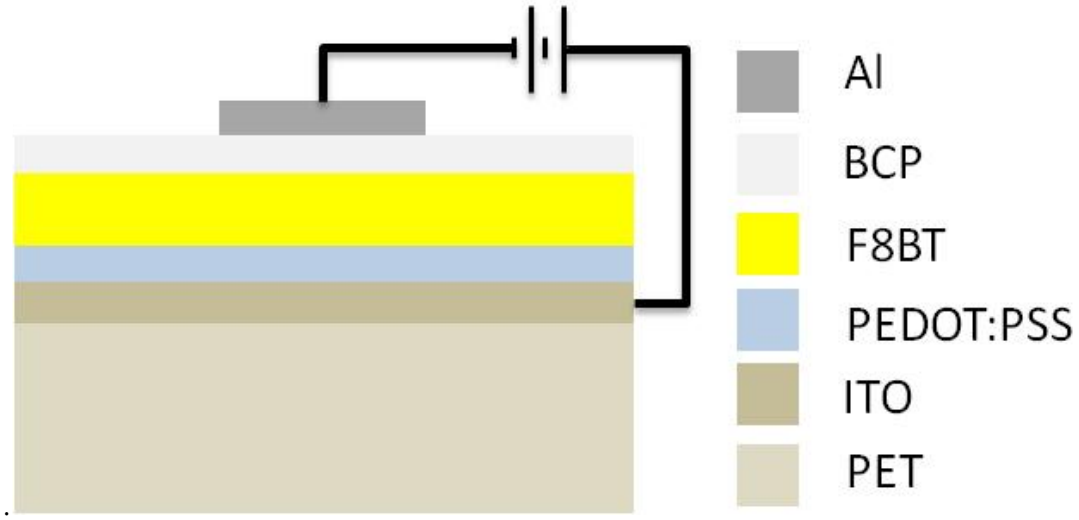

Figure 3-8: The pictorial view of the ITO/PEDOT:PSS/F8BT/BCP/Al organic diode device.

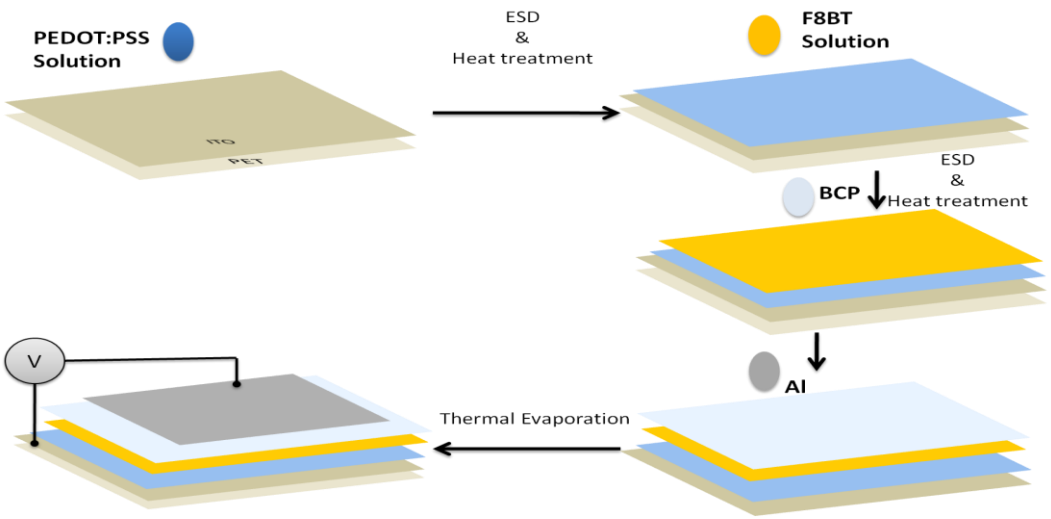

Figure 3-9: Schematic diagram illustration of the fabrication process for multi-layered F8BT OLED device having BCP as electron injection layer.

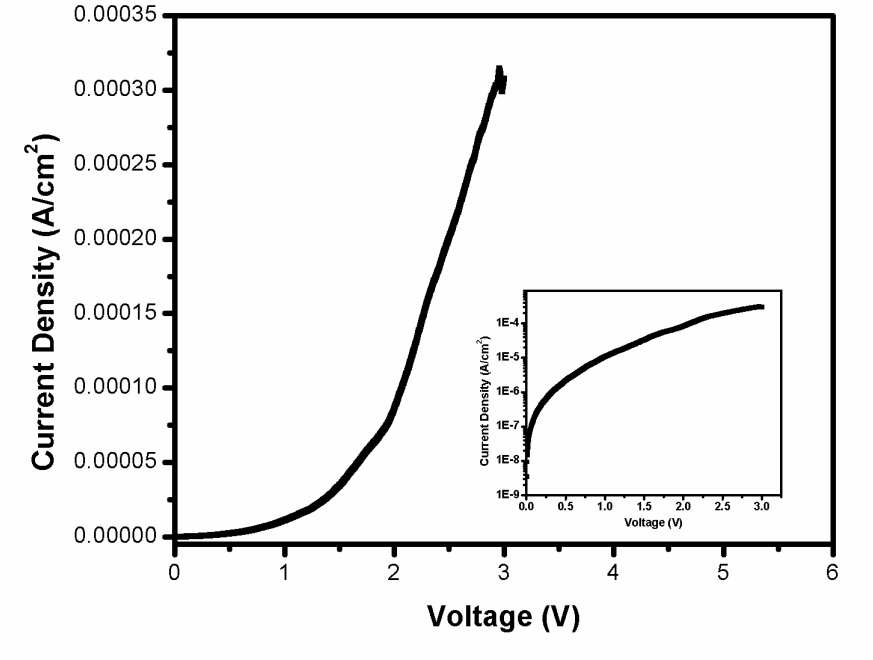

Figure 3-10: J-V characteristics of the ITO/PEDOT:PSS/F8BT/BCP/Al organic diode having deposited BCP thin film in linear scale; the inset shows J-V plot of the fabricated organic diode in semilograthimic scale.

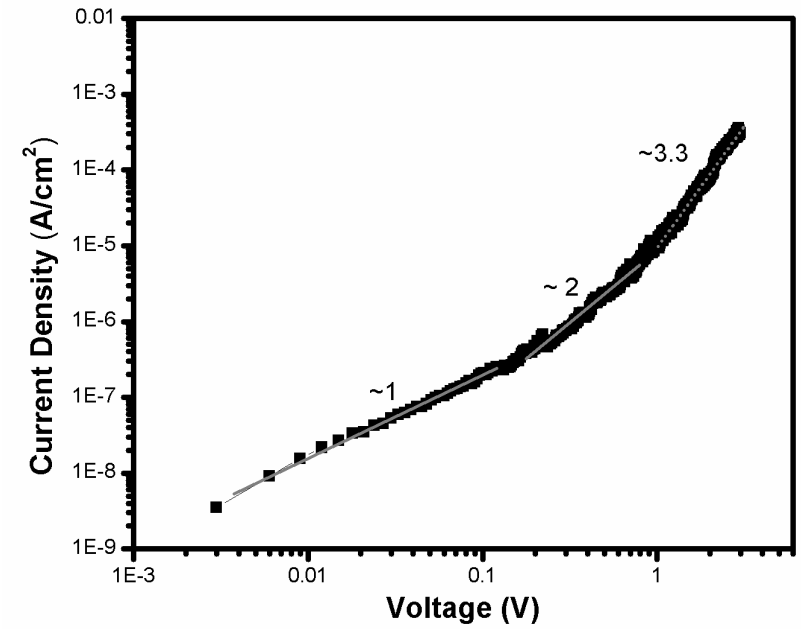

Figure 3-11: Log-Log J-V plot of the ITO/PEDOT:PSS/F8BT/BCP/Al organic diode device.

Table 4-3 shows the driving voltage of the OLED device required to generate the maximum luminous intensity of 0.1 lux. The device gave luminous intensity of 0.1 lux at the operating voltages of 20 V. The reason behind the high voltage is because of the high thickness of the BCP layer. Due to the addition of BCP layer of higher thickness, trap density probably might increase, where many electrons are trapped in the bulk. Thus, higher voltage is required to transfer the electrons to the interface of F8BT and BCP.

Table 3-3: The experimental values of luminous intensity of F8BT based OLED devices with EIL

EL Material	**Brightness (lux)**	**Voltage (V)**
F8BT (with EIL)	0.1	20

3.4 Conclusions

OLED devices based on MEH-PPV, F8BT polymeric material and F8BT along with BCP as electron injection layer have been fabricated and investigated. The electroluminescence characteristics of fabricated OLED devices were measured. The deposited MEH-PPV and F8BT showed the electroluminescence edge at wavelength of 595 and 540 nm within the visible range of light respectively. OLED devices with thin F8BT emissive layer show good current transporting properties because of proper contact between the adjacent layers in organic diode structure. This work provides a building block to achieve green and orange red light for cost effective fabrication of future full color displays.

4 Executive Summary

This thesis elucidates the optimized fabrication of ultra-flat thin-film layers of organic semiconducting materials using electrospray deposition technique. The film formation processes through ESD in detail are presented, in conjunction with any experimental data relating to process development. Detailed characterizations of functional thin films have been carried out. The thesis involves the fabrication of four different types of thin films. The thesis first discusses what organic light emitting device is and the way this technology is reshaping the microelectronics industry. The promising materials for organic electronics devices are briefly mentioned. The conventional techniques for the fabrication of thin films to be used in organic light emitting devices along with their benefits and drawbacks are highlighted. ESD as an alternative method has been introduced for organic electronics applications and its working principle, important atomization modes that is dripping, micro-dripping, unstable and stable cone jet mode and multi-jet mode along with effect of different material physical properties of the inks i.e. conductivity, viscosity, surface tension etc and effect of process parameters like electric field strength, flow rate and nozzle diameter are discussed briefly .Then the motivation of this thesis is emphasized by highlighting how ESD caters for the drawbacks of the conventional methods by its cost effectiveness and room temperature deposition process.

In the second chapter, fabrication of polymer film and small based organic thin film fabrication is presented in detail and analyses were performed thoroughly. Firstly, fabrication of thin film of poly[2-methoxy-5-(2'-ethyl-hexyloxy)-1,4-phenylenevinylene] via solution baed approach using ESD techniques being an

important material for optoelectronic devices was presented. The polymeric ink was developed and was subjected to electrostatic atomization. The ink behavior under the influence of electric field was investigated and the operating envelope of the ink was explored. The film deposited through electrospray was then characterized in physical as well as electrical aspect. Finally, the organic diode with electrosprayed polymer was fabricated. The performance of the diode device was investigated by current-voltage measurement and compared with spin-coated device. After the fabrication of functional film of the air stable Poly [9,9-dioctylfluorenyl-2,7-diyl]-co-1,4-benzo-(2,1,3)-thiadiazole (F8BT) commonly use as active layer for optoelectronic and transistor devices was discussed. Electrostatic atomization of the in-house developed F8BT polymer ink was achieved at considerable low voltage. The structural and optical characterizations of the fabricated F8BT thin film were thoroughly investigated. Furthermore, the organic diode structure with electrostatic spray deposited F8BT thin film was fabricated and its performance was analyzed by performing current voltage measurement. The current voltage characteristic curve of the organic diode showed non linear diode like behavior, thereby confirming the proper interference established between organic diode adjacent layers. The space charged limited current mechanism has been found to be dominant in the fabricated organic device with carrier mobility value of $5.65e^{-4}$ $cm^2V^{-1}s^{-1}$. Lastly, ESD as novel route to the fabrication of small molecule based 2,9-dimethyl-4,7-diphenyl-1,10-phenanthroline (BCP) organic thin film was presented and is used as buffer layer for optoelectronic devices. The tailoring of the film thickness was also performed by varying the number of deposition passes at a constant substrate speed. The structural and optical characterizations of the fabricated BCP thin film were thoroughly

investigated. The energy gap of the fabricated thin film was measured to be 3.5 eV. Furthermore, the electrical performance of the BCP thin film was verified by performing current–voltage measurement of the prototype organic diode device having fabricated BCP film as a buffer layer. The current density-voltage characteristic curve of the organic device showed non linear diode like behavior, thereby confirming the proper interference established between organic diode adjacent layers. At low voltage, the device showed ohmic conduction, where as the space charged limited current and trap charge limited current mechanism have been found to be dominant in the fabricated organic device at higher voltage.

Lastly, the detail layer by layer fabrication processes for the prototype development of organic light devices were presented. The characterizations of the fabricated flexible devices were performed and the observed results were critically discussed. OLED devices based on MEH-PPV, F8BT polymeric material and F8BT along with BCP as electron injection layer have been fabricated and investigated. The electroluminescence characteristics of fabricated OLED devices were measured. OLED devices with thin MEH-PPV and F8BT emissive layer show good current transporting properties because of proper contact between the adjacent layers in organic diode structure. This work provides a building block to achieve green light for cost effective fabrication of future full color displays. Overall, the results suggest that the electrospray deposition approach will be promising for organic light emitting devices and can be further explored for other organic semiconductor device fabrication at low cost and with low material loss. The unique advantage which ESD technique carries is that of being a much cheaper and easy solution for the

manufacture of thin film devices at standard room conditions and this thesis hence illuminates ESD as an alternative to conventional techniques.

5 Future Work

Base on the obtained results, some suggestions for future work are proposed:

- Detailed investigation of the development of thin film of organic emissive layers at different temperature for OLED applications is required to allow the device performance evaluation at different temperatures to be realized. The use of stretchable platform for polymer based devices could be beneficial for biosensing devices applications.
- The addition of dopant (Quantums, nanorods etc.) to the emissive organic layers can be investigated with the aim of producing high performance and long life durable organic electronics devices. Further, measurement and comparison of their functional properties should allow routes for the generalized controlled doping to be identified.
- Performing low temperature organic based encapsulation for the organic electronics devices is required to ensure their effect development for a variety of potential applications.

References

A. A Gringer, S. Luryi, M. R Pinto, and N. L. Schryer, IEEE T Electron. Dev., **36** , 1162 (1989).

A. Gupta, A. M. Seifalian, Z. Ahmad, M. J. Edirisinghe, and M. C. Winslet, J. Bioact. Compat. Pol. , **3** , 265 (2007).

A. Jaworek and A. Krupa, J. Aerosol Sci. **30**, 975 (1999).

A. Khan A, K. Rahman K, D. S. Kim D. S. and K. H. Choi, J. Mater. Process. Tech. , **212** , 700 (2011).

A. Khan, K. Rahman, M. T. Hyun, D. S. Kim, and K. H. Choi, Appl. Phys. A, **4** , 1113 (2011).

A. L. Shu, An Dai, H. Wang, Y-L. Loo, and A. Kahn, Org. Electron. , **14** , 149 (2012).

A. Marletta, V. Goncalves, and D. T. Balogh, Braz J Phys, 34, 697 (2004).

A. Ltaief, A. Bouazizi, J. Davenas, R.B. Chaabane, H.B. Ouada, Synth. Met. 1-3, 26 (2004).

A. Petrella, M. Tamborra, M.L. Curri, P. Cosma, M. Striccoli, P.D. Cozzoli, A. Agostiano, J. Phys. Chem., B 4, 1554 (2005).

A. R. Inigo, H.-C. Chiu, W. Fann, Y.-S. Huang, U. S.Jeng, C. H. Hsu, K.-Y. Peng, and S.-A. Chen, Synthetic. Met. , **139** , 581 (2003).

A. Swinarew, B. Piekarnik, Z. Grobelny, A. Stolarzewicz, J. Simokaitienė, E. Andrikaityte, J.V. Gražulevičius, Macromol. Symp., 308, 8 (2011).

B. C. Krummacher, V. E. Choong, M. K. Mathai, S.A. Choulis, F .So, F. Jermann , M. Zachau, Appl. Phys. Lett., **88** , 113506 (2006).

B. Chen, S. Haddad, Y. C. Wu, T. N. Fang, Z. Lan, S. Avanzino, S. Pangrle, M. Buynoski, M. Rathor and W. Cai, IEDM Technical Digest. IEEE International Conference, Washington, DC, USA, Dec. 5-5, 746 (2005).

B. Wenger, N. Tétreault, M. E. Welland and R. H. Friend, Appl. Phys. Lett. , **97** , 193303-1 (2010).

C. R. McNeill, B. Watts, L. Thomsen, W. J. Belcher, N. C. Greenham, and P. C. Dastoor, Nano Lett. , **6** , 1202 (2006).

C. Ton-That, M.R. Phillips, T.P. Nguyen, J. Lumin., 12 , 2031(2008).

C. W. Tang and S. VanSlyke, Appl. Phys. Lett. , **51** , 913 (1987).

C. Zhong, C. Duan, F. Huang, H. Wu, Y. Cao, Chem. Mater. 23(3) (2011) 326.

C.H. Park, J. Lee, J, Appl, Polym. Sci., 1 430 (2009).

D. J.Gundlach, Y. Y. Lin, T. N. Jackson, IEEE Electron. Dev. Lett. 18, 87 (1997).

D. Kabra , L. P. Lu , M. H. Song , H. J. Snaith, and R. H. Friend, Adv. Mater. , **22** , **3194** (2010).

D.H. Youn, S.H. Kim, Y.S. Yang, S.C. Lim, S.J. Kim, S.H. Ahn, H.S. Sim, S.M. Ryu, D.W. Shin, J.B. Yoo, Appl. Phys. A 4, 933 (2009).

F. Dou, and X.-P. Zhang, Chin. Phys. Lett., **28** , 097802-1 (2011).

G. Gu, P. E. Burrows, S. Venkatesh, S. R. Forrest, M. E. Thompson, Opt. Lett. 22, 175 (1997).

G. Liu, X. Zhuang, Y. Chen, B. Zhang, J. Zhu, C. X. Zhu, K. G. Neoh and E. T. Kang, Appl. Phys. Lett. **95**, 253301 (2009).

G. Susanna, L. Salamandra, T. M. Brown, A. DiCarlo, F. Brunetti, A. Reale, Sol. Energ. Mat. Sol. C , **95** , 1775 (2011).

G. Taylor, The Royal Society of London Proceedings. A. Mathematical and Physical Sciences **313**, 453 (1969).

H. F. Poon, PhD Theses, Princeton University (2002)

H. Gommans, B. Verreet, B. P. Rand, R. Muller, J. Poortmans, P. Heremans, J. Genoe, Adv. Funct. Mater. 18, 3686 (2008)

H. Ichikawa, K. Saiki, T. Suzuki, T. Hasegawa, and T. Shimada , Jpn. J. Appl. Phys. , **44** , L1469 (2005).

H. K. Jeong, Y. P. Lee, R. J. W. E. Lahaye, M. H. Park, K. H. An, I. J. Kim, C. W. Yang, C. Y. Park, R. S. Ruoff and Y. H. Lee, J. Am. Chem. Soc. **130**, 1362 (2008).

H. Spanggaard, F.C. Krebs, Solar Energy Mater. Solar Cells, 2-3), 125 (2004.

H. Xin, F. Y. Li, M. Guan, C. H. Huang, M. Sun, K. Z. Wang, Y. A. Zhang, L. P. Jin, J. Appl. Phys. 94, 4729 (2003).

H.F. Poon, D. A. Saville, I. A. Aksay, Appl. Phys. Lett. 93, 133114 (2008).

I. Hayati, A. Bailey, T.F. Tadros, Nature, 319 41 (1986).

I.B. Rietveld, K. Kobayashi, H. Yamada, K. Matsushige, J. Colloid Interface Sci., 2 639 (2006).

J. A. Lim, W. H. Lee, H. S. Lee, J. H. Lee, Y. D. Park, and K. Cho, Adv. Funct. Mater. , **18** , 229 (2008).

J. C. Wittmann, and P. Smith, Nature , **352** , 414 (1991).

J. H. Seo and C. Y. Kim J. Chem. Phys. 126, 064706 (2007)

J. Jiang, Y. Xu, W. Yang, R. Guan, Z. Liu, H. Zhen, and Y. Cao, Adv. Mater. , **18** , 1769 (2006).

J. Ju, Y. Yamagata, T. Higuchi, Adv. Mater., 43 , 4343 (2009).

J. K. Grey , D. Y. Kim, C. L. Donley, W. L. Miller , J. S. Kim , C. Silva , R. H. Friend, and P. F. Barbara, J. Phys. Chem. B, **110** , 18898 (2006).

J. M. Bharathan and Y. Yang, J. Appl. Phys. , **84** 3207 (1998) .

J. M. Shaw and P. F. Seidler, IBM J. Res. Dev. , **45** , 3 (2001).

J. Sidén, H.E. Nilsson, in: IEEE Antennas and Propagation Society International Symposium, 1745 (2007).

J. Zeleny, Phys. Rev. **3**, 69 (1914).

J.A. Ayllon, M. Lira-Cantu: Appl. Phys. A, 1, 249 (2009).

Jr. Demchuk, M. Stuke, Appl. Phys. A 61, 33 (1995).

K .Rahman, J. B. Ko, S. Khan, D. S. Kim, and K. H. Choi, J. Mech. Sci. Technol. , **1** , 307 (2010).

K. H. Choi, A. Ali, A. Rahman, N. M. Mohammad, K. Rahman, and A. Khan, D. Kim, J. Micromech. Microeng. **20** , 075033 (2010).

K. H. Choi, M. Mustafa, J. B. Ko, Y. H. Doh, Thin Solid Films 525, 40 (2012).

K. Jong Lee, B. Ho Jun, T. Hoon Kim, J. Joung, Nanotechnol., 17 (2006) 2424.

K. M. Vaeth, Inform. Display 19, 12 (2003).

K. Rahman, A. Khan, N.M. Nam, K.H. Choi, D.S. Kim, J. Precis. Eng. Manuf. 4 663 (2011).

K.E. Paul, W.S. Wong, S.E. Ready, R.A. Street, Appl. Phys. Lett., 83, 2070 (2003).

K.H. Choi, M. Mustafa, K. Rahman, B.K. Jeong, Y.H. Doh, Appl. Phys. A, 106 ,165 (2011).

L. J. Cote, F. Kim and J. Huang, J. Am. Chem. Soc. **131**, 1043 (2008).

L. L. Chua, J. Zaumseil, J. Chang, E. C. Ou, P.K. Ho, H. Sirrnghaus and R.H. Friend, Nature , **434** , 194 (2005).

L. L. G. Justino, M. L.Ramos, P. E. Abreu, R. A. Carvalho, A.J. F. N. Sobral, U. Scherf, and H. D. Burrows, J. Phys. Chem. B , **113 ,** 11808 (2009).

L. Zhao, Z.L. Zhou, Z. Guo, J. Pei, S. Mao, MRS Proc., (2011) DOI: 10.1557/opl.2011.884

L.-C. Chao, F.-C. Tsai, and J.-C. Su, Mat. Sci. Semicon. Proc., **11** , 13 (2008).

M. Campoy-Quiles, G. Heliotis, R. Xia, M. Ariu, M. Pintani, P. Etchegoin, and D. D. C Bradley, Adv, Funct. Mater. , **15** , 925 (2005).

M. Friedman, and G.Walsh, Polym. Eng. Sci. , **42** , 1756 (2002).

M. Kertesz, C.H. Choi, S. Yang, Chem. Rev., 10, 3448 (2005).

M. Prelipceanu, O.-G. Tudose, O.-S. Prelipceanu, S. Schrader, and K. Grytsenko, Mat. Sci. Semicon. Proc. , **10** , 24 (2007).

M. S. P. Sarah, M. Z. Musa, A. B. Suriani, N. S. Jumali, Z. Shaameri, A. S. Hamzah and M. Rusop, in: Proceedings Semiconductor Electronics (ICSE 2010) Melaka, Malaysia, 2010, 2010 IEEE International Conference, 241 (2010).

M. Shtein, J. Mapel, J. B. Benziger, S. R. Forrest, Appl. Phys. Lett. 81, 268 (2002)

M.K. Fung, S. L. Lai, S.W. Tong, S.N.Bao, C.S. Lee, W.W. Wu, M. Inbasekaran, J. J. O'Brien, and S.T. Lee, J Appl. Phys., **94** , 5763 (2003).

M.-Y. Lee, M.-W. Lee, J.-E. Park, J.-S. Park and C.-K. Song, Microelectron. Eng. , **87** , 1922 (2010).

N. Duraisamy, N. M. Muhammad, A. Ali, J. Jo, K. H. Choi, Mater. Lett. 83, 80 (2012).

N. Kamarulzaman, N.D.A. Aziz, R.H.Y. Subban, A.S. Hamzah, A.Z. Ahmed, Z. Osman, R. Rusdi, N. Kamarudin, N.S. Jumali, Z. Shaameri, in: 3rd International

Symposium & Exhibition in Sustainable Energy & Environment, Melaka, Malaysia, 2011 ,63 (2011).

N. M. Muhammad, A. M. Naeem, N. Duraisamy, D. S. Kim, and K. H. Choi, 1751 Thin Solid Films, **520** , 1751 (2011).

N. M. Muhammad, S. Sundharam, H.W. Dang, A. Lee, B.H. Ryu, K.H. Choi, Curr. Appl. Phys., 11(1-1), S68 (2011).

N. Rehmann, D. Hertel, K. Meerholz, H. Becker, S. Heun, Appl. Phys. Lett., 91, 103507 (2007).

O. Lavastre, I. Illitchev, G. Jegou, P.H. Dixneuf, J. Am. Chem. Soc. 19, 5278 (2002).

O.V. Kim, P.F. Dunn, Langmuir, 26, 15807 (2010).

P Miao, W. Balachandran, and P. Xian, Magazine IEEE , **3** , 46 (2001).

P. Cea, Y. Hua, C. Pearson, C. Wang, M. Bryce, F. Royo, M. Petty, Thin Solid Films 1-2 , 275 (2002).

P. Leclere, M. Surin, P. Brocorens, M. Cavallini, F. Biscarini, and R. Lazzaroni, Mater. Sci. Eng. , **R 55**, 1 (2006).

P. Peumans, S. R. Forrest, Appl. Phys. Lett. 79, 126 (2001).

P. Peumans, S. Uchida, S. R. Forrest, S. R. Nature 425, 158 (2003).

P. Peumans, V. Bulovic´, S. R. Forrest, Appl. Phys. Lett., 76, 2650 (2000).

P.R. Andres, U.S. Schubert, Adv. Mater., 13, 1043 (2004).

Q. L. Song , F. Y. Li , H. Yang , H. R. Wu , X. Z. Wang , W. Zhou , J. M. Zhao , X. M. Ding , C. H. Huang, X. Y. Hou, Chem. Phys. Lett. 416, 42 (2005).

R. Bakhshi, M. J. Edirisinghe, A. Darbyshire, Z. Ahmad and A M. Seifalian, J. Biomater. Appl., **4** ,293 (2009).

R. Hartman, D. Brunner, D. Camelot, J. Marijnissen, and B. Scarlett, J. Aerosol Sci. , **1** , 65 (2000).

R. Hartman, D. Brunner, D. Camelot, J. Marijnissen, B. Scarlett, J. Aerosol Sci. 1, 65 (2000).

R. K Gupta and R. A. Singh, Mat. Sci. Semicon. Proc., **7** , 83 (2004).

R. K. Gupta, K. Ghosh, P.K. Kahol, J. Yoon, and S. Guh, Appl. Surf. Sci. , **254** , 7069 (2008).

R. Parashkov, E. Becker, T. Riedl, H. H. Johannes and W. Kowalsky, Proceedings IEEE **93**, 1321 (2005).

R. Taylor, K. Church, M. Sluch, Displays, 2 ,92 (2007).

R. U. A. Khan, C. Hunziker, P. Günter , J Mater Sci: Mater Electron. 17, 467 (2006).

S. A. DiBenedetto, A. Facchetti,. M. A. Ratner and T. J. Marks, Adv. Mater., **21** , 1407 (2009).

S. C. Chang, J. Liu, J. M. Bharathan, Y. Yang, J. Onohara and J. Kido, Adv. Mater. , **9** , 734 (1999).

S. C. Chang, J. M. Bharathan, Y .Yang, R. Helgeson, F. Wudl, M. B. Ramey, and J. R. Reynolds, Appl. Phys. Lett. , **73** , 2561 (1998).

S. Cook, PhD Theses, Chemistry Department , Imperial College London (2006).

S. Di Risio, N. Yan, Macromol. Rapid Commun., 18-19 , 1934 (2007).

S. Gil Kim, K. Hyun Choi, J. Hwan Eun, H. Joon Kim, C. Seung Hwang, Thin Solid Films, 377 ,694 (2000).

S. Ilkhanizadeh, A.I. Teixeira, O. Hermanson, Biomaterials, 27, 3936 (2007).

S. Jayasinghe, M. Edirisinghe, Journal of the European Ceramic Society, 8, 2203 (2004).

S. Jeong, W.-H. Jang, and J. Moon, Thin Solid Films, **466** , 204 (2004).

S. Kumar, T. Nann, J. Mat. Res., 19, 1990 (2004).

S. Li, E. Kang, Z. Ma, K. Tan, Surf. Interface Anal. 2 ,95 (2000).

S. R. Forrest, Nature 428, 911 (2004).

S. Varghese, M. Iype, E. J. Mathew, C.S. Menon, Mater. Lett. 56, 1078 (2002).

S. Vázquez-Córdova, G. Ramos-Ortiz, J.L. Maldonado, M.A. Meneses-Nava, O. Barbosa-García, Revista Mexicana De FÃsica, E 2, 146 (2008).

S. Westenhoff, I. A. Howard, J. M. Hodgkiss, K. R. Kirov, H. A. Bronstein, C. K. Williams, N. C. Greenham, and R. H. Friend, J. Am. Chem. Soc. , **130** , 13653 (2008).

S.A. Arnautov, E.M. Nechvolodova, A.A. Bakulin, S.G. Elizarov, A.N. Khodarev, D.S. Martyanov, D.Y. Paraschuk, Synth. Met. 1-3 ,287 (2004).

S.A. Jenekhe, S.B. Schuldt, Ind. Eng. Chem. Fundamen., 4 , 432 (1984).

T. Fukuda, T. Suzuki, R. Kobayashi, Z. Honda, and N. Kamata, Thin Solid Films, **518** , 575 (2009).

T. Ito, Y. Okayama, and S. Shiratori, Thin Solid Films, **393** , 138 (2001).

T. Nguyen, E. Djurado, Solid State Ionics, 3 191 (2001).

T.P. Nguyen, Mat. Sci. Semicon. Proc. , **9** , 198 (2006).

T.S. Kang, B.S. Harrison, T.J. Foley, A.S. Knefely, J.M. Boncella, J.R. Reynolds, K.S. Schanze, Adv. Mater. 13 1093 (2003).

T.W. Yoo, C. Park, N.T. Mai, D.U. Kim, L.S. Park, Molecular Crystals and Liquid Crystals, 1 69 (2011).

W. Lee, G. Choi, Y. Seo, Phys. Status Solidi (c) 10 3401 (2008).

W. Stampor, A. Tykocki-Piłat, Photonics Lett. Pol. 3 (2), 64 (2011).

W.W. Flack, D.S. Soong, A.T. Bell, D.W. Hess, J. Appl. Phys., 4 1199 (1984).

X. D. Zhuang, Y. Chen, G. Liu, P. P. Li, C. X. Zhu, E. T. Kang, K. G. Noeh, B. Zhang, J. H. Zhu and Y. X. Li, Adv. Mater. **22**, 1731 (2010).

X. Zhao, , C. Hinchliffe., C. Johnston, P. J. Dobson, and P. S. Grant, Mat. Sci. Eng. B, **151** , 140 (2008).

Y. Liu, T. Cui, K. Varahramyan, Solid-State Electronics, 9 (2003) 1543.

Y. Zhang, P. and W. M. Blom, Appl. Phys. Lett., **98** , 143504-1 (2011).

Z. T. Liu , C. Y. Kwong , C. H. Cheung, A. B. Djurisic ,Y. Chan, P. C. Chui, Synthetic Met. 150, 159 (2005).